Rapid Single-Cell Electroporation for Labeling Organotypic Cultures

by

Joseph D. Steinmeyer

B.S.E Electrical Engineering (2008)

University of Michigan, Ann Arbor

MASSACHUSETTS INSTITUTE OF TECHNOLOGY

JUL 12 2010

LIBRARIES

ARCHIVES

Submitted to the Department of Electrical Engineering and Computer Science
in Partial Fulfillment of the Requirements for the Degree of
Master of Science in Electrical Engineering and Computer Science

at the

Massachusetts Institute of Technology

June 2010

© 2010 Massachusetts Institute of Technology
All rights reserved

Signature of Author_____
Department of Electrical Engineering and Computer Science
April 30, 2010

Certified by_____
Mehmet F. Yanik
Associate Professor of Electrical Engineering and Computer Science
Thesis Supervisor

Accepted by_____
Professor Terry P. Orlando
Chair, Department Committee on Graduate Students

Rapid Single-Cell Electroporation for Labeling Organotypic Cultures

by

Joseph D. Steinmeyer

Submitted to the Department of Electrical Engineering and Computer Science
On April 30, 2010 in Partial Fulfillment of the
Requirements for the Degree of Master of Science in
Electrical Engineering and Computer Science

ABSTRACT

Single-cell electroporation is a technique for transfecting individual cells in tissue culture at relatively high efficiencies, however it is both time-consuming and low-throughput and this limits the number of different labeling agents that can be effectively introduced into a region of tissue in reasonable periods of time. A novel system that will rapidly load, clean, and accurately position a glass micropipette electrode into tissue culture for single-cell electroporation is proposed. The system will significantly increase the number of different labeling agents that can be introduced into a single tissue culture per unit time. This in turn, will provide a means for improving the study of neural anatomy at cellular resolutions in both tissue culture and *in vivo* environments.

Thesis Supervisor: Mehmet F. Yanik
Title: Associate Professor of Electrical Engineering and Computer Science

CONTENTS

1. INTRODUCTION

A growing trend in neuroscience over the last decade has been a move away from research conducted as *in vitro* cell studies and towards research conducted as *in vivo* (whole organism) studies. Much of this motivation comes from the inherent fact that the nature of what makes neural systems complete is not just the single neuron but how each neuron is affected by and affects other neurons; the network is what counts. Studying neurons outside of the network will ultimately provide only a limited amount of information about how the nervous system functions. The next steps in pursuing and understanding almost all fundamental questions in neuroscience will involve studying the neurons as they relate to one another in their native environment in the organism.

At the same time, in the past decade significant research has begun to show the importance of non-neuronal cell function in the nervous system. Glial cell types such as astrocytes, oligodendrocytes, microglia, ependymal cells, and others, which were originally dismissed as "support cells", are now known to carry out functions far more complex than ever imagined twenty years ago[1]. Consequently, the study of dissociated neurons in the absence of glial cells is now called into question or viewed as invalid for some sub-areas of neuroscience research. For example, studying the affect of drugs on dissociated neurons has been shown to be significantly different between dissociated *in vitro* neurons and neurons studied *in vivo*[2].

Unfortunately, conducting *in vivo* studies brings with it a significant battery of problems and difficulties which do not exist with *in vitro* techniques. Firstly, generating stable transgenic animal lines, one of the most common means of genetic manipulation in higher organisms such as mouse and rat for *in vivo* studies, can be very time-consuming and require large amounts of infrastructural resources. Maintaining transgenic lines of mice for the purpose of screens can be taxing both financially and logistically[3], and minimization of the usage of animals in tests and screens is a recent trend in many circles[4]. While it would be wonderful to study the brain in its native environment, notably in its intact form inside the living organism, *in vivo*, it is extremely difficult, if not impossible, due to limitations in imaging and other techniques, with two-photon imaging having depth limitation of approximately 300 μm of tissue[5]. Physical manipulation of cells and tissue in such an environment is also limited. A sort of Catch-22 exists where one needs to study the intact brain, but in order to do so the brain needs to be broken down, violating the original requirement. In order gain access to these complex systems, they must be broken down, but in doing so the complex structure and inter-reliance of the cells may start to be lost resulting in an altered system. At the level of dissociated cells, systems-level work is exceedingly difficult to justify because the native system is no longer present.

A potentially suitable middle ground between purely *in vivo* and purely *in vitro* studies for many neuroscience studies could involve organotypic slice culture, which is a means of maintaining carefully dissected slices of tissue in artificial neural environments for many weeks[6]. Organotypic slice culture can find its roots in research as early as the 1940's[7] although it wasn't until the early 1980's that organotypic culturing became well-characterized and a reliable method with which to conduct research[8, 9]. Furthermore, culturing of tissue on membrane inserts[10] as opposed to the original roller-tube method[8] has allowed the tissue to be more readily worked on in conjunction with conventional microscope and electrophysiology techniques. Current methods

and protocols[6, 11, 12] make culture of organotypic neural tissue, particularly the hippocampus, a relatively simple and reliable technique, and significant work has been carried out on differences between slice anatomy and actual *in vivo* anatomy that allow for a good conceptual bridge to connect findings from one to the other. Hippocampal organotypic cultures possess/maintain many features which make them attractive candidates for the study of neural function at both the cellular and system level. Particularly, CA1 cells in hippocampal organotypic cultures have been shown to be relatively stable and similar to their true *in vivo* counterparts over large periods of time[13].

While organotypic cultures provide a convenient and powerful platform through which to study neural function in a quasi *in vivo* format, and in fact significant findings have come from transfection and electrophysiology recordings done with the cells in such cultures, they are still not being used to their full potential as a biological platform due to technological limitations. Most work in organotypic slices is still painfully manual, including localized transfections through single-cell electroporation[14]. If the scientific community is to continue to make advances by using organotypic cultures as a research platform, novel ways to transfect, image, manipulate, and sample at single-cell accuracy must continue to be developed and perfected.

Driven by this need, we set out to develop a system which could allow the transfection of a wide library of labeling agents at single-cell accuracy into organotypic slices at high speed. The system designed combines both traditional single-cell electroporation techniques and well established tissue culture techniques with significant levels of automation and computer programming. Additionally, entirely new techniques for small volume sampling in conjunction with single-cell electroporation all combine together to allow the rapid and efficient transfection of multiple labeling agents in organotypic slices. The presented thesis therefore discusses the work carried out in the development of this system, including initial designs through to actual implementations and proof of concept.

2. A Brief Overview of Transfection Methods in Organotypic Cultures

Numerous techniques exist for introducing genetic and other components into cells in cultured slices, and each possess unique benefits and downsides. A brief overview of the major techniques is discussed below.

2.1 Viral Labeling

Introducing genetic material into single cells using viruses has become more popular in recent years as control and design of viruses has improved. The introduction of several new varieties of viruses for transfection including HSV (Herpes Simplex Virus) have further increased the robustness of the procedure[15, 16]. For labeling in cultured tissue, two general approaches are used: The first relies upon localized injection of the virus[17, 18] where a micropipette loaded with the virus deposits a quantity of the viruses onto the tissue culture. This can reliably label cells within a confined region. The second method is washing the entire tissue sample in a low-titer bath of the virus and relying upon stochastic labeling.

In both cases, since the viruses can often specifically target neural populations by utilizing surface markers of the cells, astrocyte or other support cell labeling is kept to a minimum. Both variants of the technique are relatively easy to implement, and as mentioned above, virus design has become more reliable in recent years. However, viral labeling does not permit single-cell accuracy in labeling cells. Based on conditions, for example, one could expect viral labeling of approximately ten cells per brain slice, but it is effectively impossible to determine ahead of time which specific cells will be transfected. This single fact limits the usage of viruses in cells in tissue culture in some cases.

2.2 Microinjection

Single-cell microinjection allows a user to transfect into a single cell with a relatively high survival rate. Glass capillary micropipettes with resistances on the order of 20 to 40 MΩ are produced, loaded with labeling agents such as fluorescent dyes or plasmids, and used to inject the cell under visual control[19]. Depending on conditions, injection of the nucleus may be needed required for successful transfection. For very high resistance tips, it can be exceedingly difficult to rear-load the sample, and occasionally front-loading must be used[20].

Such a technique provides the benefit of accurately targeting single cells in tissue culture; in other words, the user knows exactly which cells are targeted, something which is not an option when using viral transfections. Single-cell microinjection is an inherently low-throughput technique, however, often times requiring a change in microcapillary pipette after only ten or fifteen injections due to the extremely narrow geometric parameters of the tip and the inherent fact that the tip is forcefully rammed into the cell membrane. Once the tip is clogged, the hydraulic resistance can be so high that even very high pressures cannot have an effect; the gaskets holding the pipette will fail before the clogged cell debris is removed. The only course of action is to change the micropipette, an inherently time-consuming and low-throughput process.

2.3 Opto-Transfection

Opto-transfection, also known as optoporation, is a relatively new transfection technique which involves the application of highly focused short-pulse laser radiation on or near a cell in order to generate pores in the cell's membrane[21]. While such a method has been shown theoretically and experimentally to result in relatively high transfection efficiencies[22], it still only provides a mean to penetrate the barrier of the cell membrane and not simultaneously introduce agents, something which must still be done using injection micropipettes, which are prone to clogging as mentioned above. Consequently it is not as of yet a very useful technique for transfecting cells in tissue culture.

2.4 Electroporation

Electroporation relies on the well-known phenomenon that when the voltage across a cell's membrane exceeds a certain threshold level, with values ranging anywhere from 200 mV to 1.0 V, the membrane reorganizes itself and forms pores[23]. (Note that this should not be confused with dielectric breakdown of the membrane which is an entirely different physical process.)

Electroporation has been a firmly-established technique for transfecting large numbers of bacteria with plasmids and other materials for decades[24, 25]. Usage with free-floating eukaryotic and even mammalian cells was developed more recently, and the last ten years have seen the emergence of on-chip technologies for electroporation[26, 27]. Electroporation via large conductive pads it is also used as a technique for transfecting embryos when generating transgenic lines in animals[28]. Some researchers have also used what we term "bulk electroporation" for localized labeling or dye uptake in the eyes of chick embryos[29]. Electroporation as demonstrated in all of these examples is not compatible with organotypic culture, and must be modified to be of use. A more specialized sub-field of electroporation, known as single-cell electroporation (SCE) is one of the primary topics of this paper. Details on the technique are discussed below, but it is important to emphasize that while the same physical phenomena are at work in both general "bulk" electroporation and SCE, the actual equipment utilized is far different.

3. The Current State of Single-Cell Electroporation

Single-cell electroporation, as its name clearly implies, is a means of electroporating a single cell for the purpose of introducing a labeling agent, protein, or genetic element. It has only been in the past ten years that successful, repeatable, and efficient electroporation with single-cell resolution has been obtained in such a way to prove itself as an important tool in biology[30]. Original efforts relied upon pairs of carbon fiber electrodes placed around isolated single cells located in salt-solution baths containing the transfection agents of interest[24, 31, 32]. This work was soon followed by single-micropipette electroporation with single-cell resolution in dissociated cells and tissue cultures[33] as well as *in vivo*[34]. The specific technique has been improved upon more recently[35-38] and significantly characterized for different agents[39] to the point where it is now a reliable method to accurately transfect single or small groups of cells *in vitro*, *in vivo* , and in tissue cultures. Recently, researchers were even able to successfully introduce small interfering RNA with single-cell resolution into cell cultures by single-cell electroporation, providing a convenient method for silencing the expression of genes at a single-cell resolution[40]. While this was successfully been demonstrated in cerebellar cell cultures, it has not been shown in organotypic brain slices as of yet.

The basic format for modern SCE is depicted in Figure 1. The tip of a salt-filled pulled-glass micropipette containing the transfection agent is positioned close to the membrane of the cell which is to be transfected. A voltage source, generally computer controlled, drives a signal into the pipette, and the resultant electric field at the tip porates the membrane of the cell. Either a pressure-driven flow, electrophoretic flow, electroosmotic flow, or a combination of these three phenomena simultaneously drives the diffusion of transfection agent(s) into the cell. In the case of genetic elements, the transfection agents must also be taken up by the nucleus, and the details of this process are still a matter of debate[41]. It has in fact been noted by some researchers that the pores generated in SCE can stay open for a matter of minutes following applications of pulses, and that for large molecules such as plasmids, other yet-to-be-described processes are involved in uptake rather than the assumed method of diffusion through pores[14, 42]. As becomes apparent when surveying the literature on SCE, there can be noticeable variations from this basic SCE format from research group to research group.

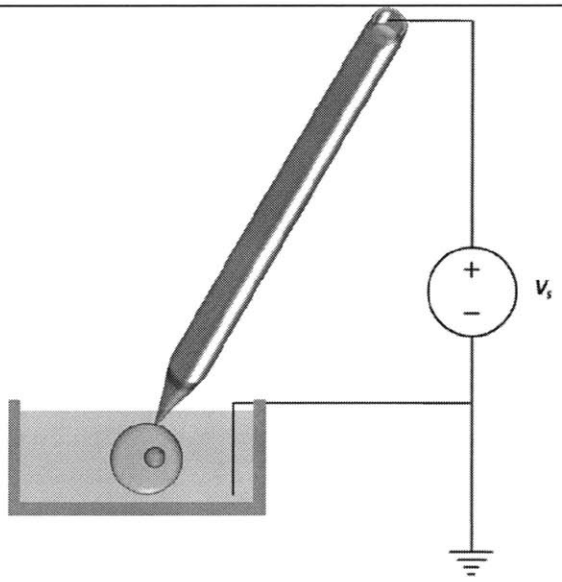

Figure 1| The standard setup for modern single-cell electroporation (SCE). A voltage signal is applied to salt-filled pulled-microcapillary via a silver-chloride wire. The salt solution conducts the signal down to the tip of the microcapillary and the resultant electric field generates pores in the membrane of the cell which permit the transfection agents, driven by pressure, electroosmotic, or electrophoretic flows, to rush into the cell and/or nucleus.

Technologically speaking, SCE can be carried out using almost no additional equipment to what is normally found in a standard electrophysiology rig. The only exception may be a voltage amplifier of sufficient bandwidth, although even this may not be necessary depending on what is being transfected. At least one commercialized SCE device has been developed and released, namely the Axoporator sold through Molecular Devices with a price tag in the neighborhood of $8,000. Important to the purpose of this thesis, it should be emphasized that SCE carried out in this manner, is a very-low throughput technique requiring manual loading of agents into micropipettes and continuous calibration and adjustment of the setup for successful operation.

There have been some attempts at the development of valid models for simulation of SCE at various voltages, currents, and frequencies[43-45], however these are only reliable in cases of isolated cells, and in general it is accepted that they are not valid in the heterogeneous environment of tissue slice cultures. As a result, the voltage, current, and frequency of the signals applied for SCE in tissue culture is usually derived through a trial-and-error process by the researcher.

3.1 Limitations

If one reads any papers on single-cell electroporation, tip clogging is often listed as the number one troubleshooting point in running the system. Like with any micropipette technique placing the small-bore glass opening near cells increases the chances a piece of debris will clog the tip. While this can be a significant problem when working with single dissociated cells[44], when working in tissue culture and *in vivo* conditions where extracellular material is excessive, clogging can become debilitating, and significant effort is put into applying certain pressure

levels[36], using distinctive pulse shapes[14], or tightly controlling approach angles in order to minimize the chance for clogging the tips. Despite all of these techniques, clogging does occur in standard SCE, and does so with significant regularity. As shown in Figure 2, clogging of the tips with cellular debris can be detected using both visual methods and by analyzing the current trace from applying known pulses to the tip, but even this is not enough, as discussed below in this thesis.

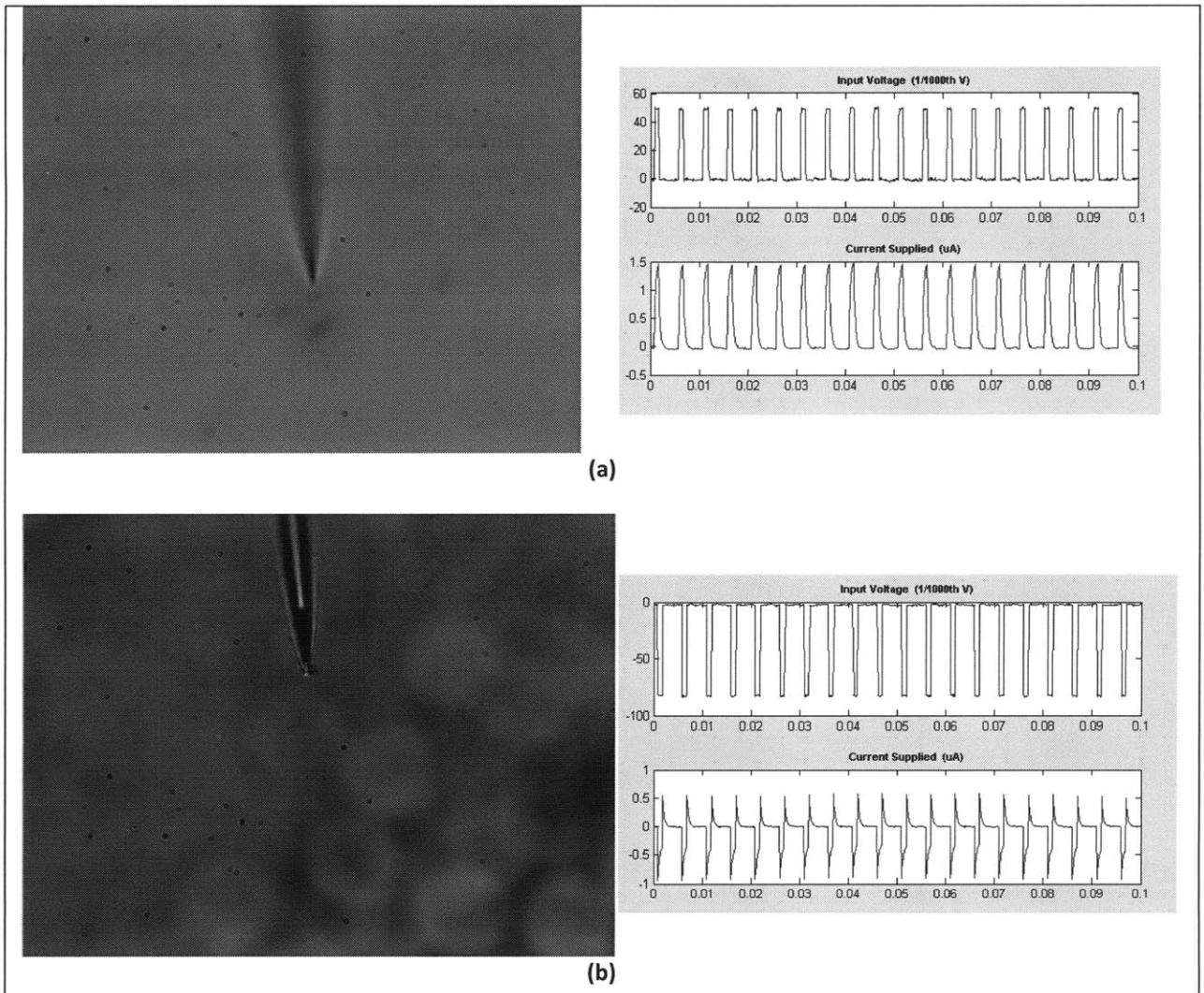

Figure 2| A significant issue when carrying out SCE in tissue culture is clogging of the tip from cellular debris. By measuring the current through the electroporation system as a function of time, the viability of the tip can be easily determined. A functional, clear pipette tip will yield distinctly clear and uniform RC time constants indicative of a dominant parallel capacitance in the system is shown in **(a)** above. When the tip becomes clogged from debris, the user can occasionally note the impaired electrical contact through visual means (see the discontinuity in the tip and the dangling debris at the tip of the micropipette in the left of **(b)**), however an additional reliable method involves the plot of current taking on the characteristic of a resistor *in series* with a capacitance with approximately equal swings in current for both polarities.

Often, when the tip does clog, it is simply thrown away, and what little of the sample that can be saved will be withdrawn. This approach to SCE is inherently wasteful, time consuming, and not

conducive to high-throughput technology. The author spent significant time recreating standard manual SCE, and it became apparent where the largest amounts of time are lost: particularly, the actual transfection portion of an SCE procedure with a loaded pipette in tissue can be easily carried out at 20 cells/minute or higher depending on labeling density. The bulk of a researcher's time is spent in loading the micropipette, positioning it, and verifying its electrical and fluidic integrity, all of which can easily take five minutes on each attempt. Every time a new agent needs to be introduced, five minutes of prep time at least is required.

In order to gain single-cell accuracy in SCE, a system with sufficiently high magnification and resolution is required. Several groups have carried out SCE using stereomicroscopes[34], but this is only valid when targeting large neurons in visible places or when single-cell accuracy is not needed. As it has turned out, the water immersion objectives found on many electrophysiology microscopes are a good choice for SCE in tissue culture due to their high NA and relatively large working distances, and the fact that the thickness of the slice prevents clear bright-field imaging from below. Water-immersion objectives do however impose strict geometric restrictions on approach angle, size of the pipette, taper of the pipette, and many other things which are detailed in sections of this thesis below.

The currently inherently low-throughput nature of SCE in tissue culture limits the number of different labeling agents that can be administered in a slice in a given period of time. A researcher can easily transfect twenty cells with a single small molecule dye such as Alexa Fluor 488 in five minutes, but to do two different dyes in the same brain slice would require at least fifteen minutes. Keeping organotypic cultures outside of incubators for much longer than this will begin to result in a decrease in slice survival.

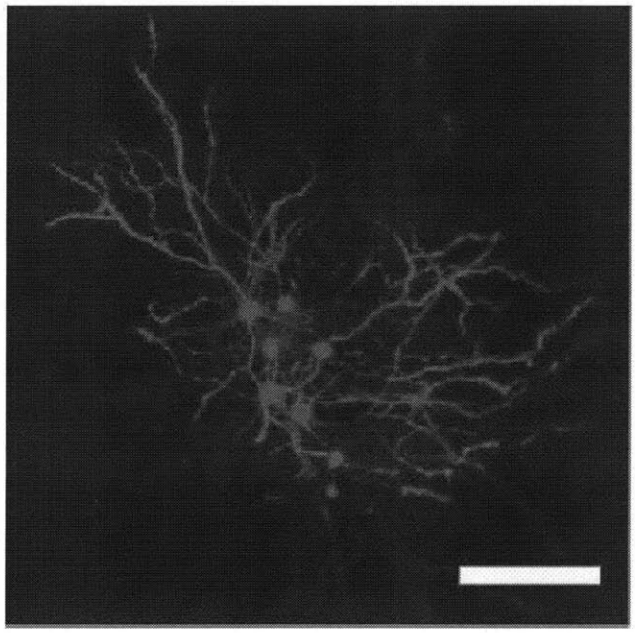

Figure 3| SCE of a single fluorophore-encoding plasmid for the purpose of labeling and neurite tracing is a readily implemented technique for organotypic cultures but transfecting multiple cells makes tracing of individual processes extremely difficult [37]. As a result, labeling must be done at low densities in order to avoid overlapping and possible confusion in tracing. Scale bar is 100 μm.

3.2 A Proposal to Overcome Current Limitations

After analyzing current techniques and shortcomings in SCE, it was determined that the weak-link in using current SCE techniques for higher-throughput purposes in cultured tissue slices is the amount of preparation time required for loading, positioning, and calibrating the micropipette tips. If this portion of the technique could be automated, it would be possible to drastically decrease the time, the resources, and the variability in transfection, and consequently increase the number of different agents that can be reliably transfected into a tissue culture slice in a given period of time.

In order to achieve this end-goal, four novel techniques were developed:

1. Front-loading of micropipette: Rear-loading of micropipettes wastes large quantities of sample, and is a time-consuming process which must be repeated for each agent transfected. Diffusion-controlled front-loading of salt-solution-filled micropipettes was developed as a means to greatly decrease the volume of agent needed and the time required for loading.

2. Rapid cleaning of micropipette: Front-loading of samples can be repeatedly carried out on the same micropipette if a reliable technique for cleaning the pipette between different agents is developed. Additionally, tip-clogging, which is normally an irreversible fault-point for traditional SCE can be overcome by using specialized cleaning techniques discussed in this thesis.

3. Automated position control of micropipette, tissue culture, sample library, and cleaning units: A set of software controls all mobile aspects of the system in order to ensure rapid and fault-free operation of the critical and delicate components of the system. Doing so greatly increases reliability compared to when human-control is primarily used.

4. Fixed-position micropipette and mobile tissue culture: In order to increase the reliability of micropipette positioning, the opposite approach to cell-targeting was developed for use in the system. Instead of moving the micropipette towards the cell of interest, the micropipette is constantly kept in the plane-of-focus in the system, and the tissue culture, mounted on a three-axis stage is moved towards the micropipette for targeting.

The details of the development and implementation of these techniques will be discussed in the sections below.

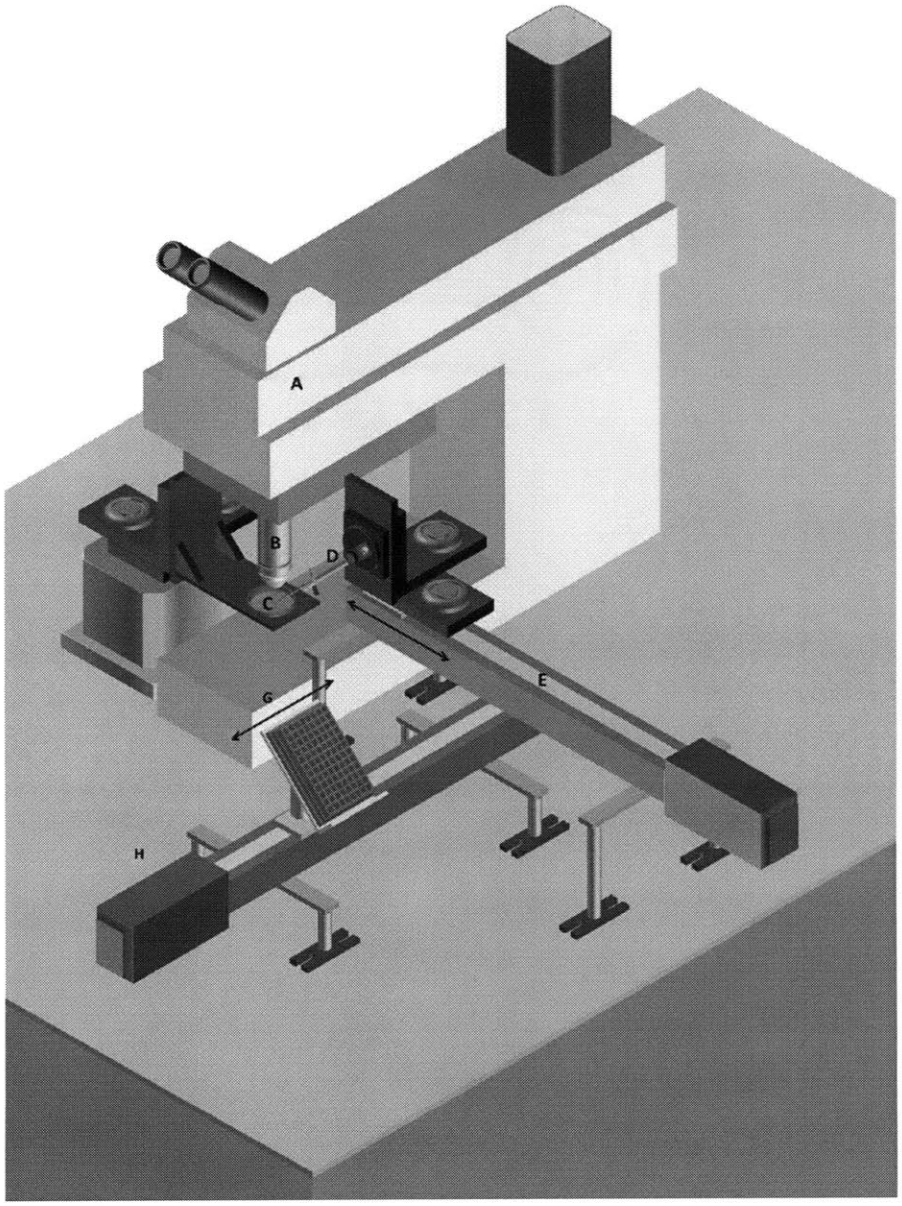

Figure 4| Overall image of the high-throughput organotypic brain slice transfection system presented in this thesis. The system is built around an upright electrophysiology microscope (**A**), containing a 16× 0.8 NA water-immersion objective (**B**). The tissue culture is placed in a heated bath controlled by a three-axis stage (**C**). A glass micropipette mounted on a micromanipulator (**D**) is used to carry out SCE on the tissue slice under visual control from the user. When the user wishes to transfect a new compound, the entire micromanipulator assembly is backed away from the microscope on a linear-stage (**E**), and the micropipette tip can be washed and loaded from a modified well-plate (**G**) with a new compound by a perpendicular long-travel linear stage (**H**). Each sub-system is discussed below in detail including development and choice of microscope, development of software, development of automation and similar considerations, work with micropipette design, and objective lens compatibility. A photograph of the actual setup is presented in Appendix B.

4.1 Equipment and Hardware

The entire system is built around a Nikon FN-1 Electrophysiology microscope possessing a 16× 0.8 NA objective and is capable of three primary imaging techniques: differential interference contrast (DIC), epi-fluorescence, and brightfield imaging. A variety of cameras were used at various points in the development of the system including a 1024×1017 pixel EMCDD (Andor), a 600×800 color camera (MVC), and 640×480 analog video camera (Hamamatsu), and a 1024×1024 cooled camera (Photometrics CoolSNAP). A custom-built two-photon imaging system comprised of scan mirrors (Cambridge Technologies), optical equipment and hardware (Thorlabs) filters (Omega), and a H3478 photomultiplier tube (Hammatsu) was also incorporated into the system, however it was not used significantly in the work presented in this paper. Some details on the two-photon setup can be found in an additional publication by our group[46]. The microscope is also equipped with a gimbaled-mirror and magnification changer which permits effective magnifications of 5.6×, 32×, and 64× at any portion of the main field of view.

A pair of two micromanipulators (Sutter MP 285) are used to provide tissue sample movement in three directions (modified with Sutter stage adapter 3DMS) and micropipette movement in three directions. Both of these micromanipulators have 25 mm of travel range in all three axes with 62.5 nm step-size and are driven simultaneously through a Sutter MPC-2000FN control system. The stage is temperature-controlled (Harvard Apparatus TC-344B) using a compatible slice bath.

Micropipettes were pulled from a variety of capillary glass including primarily filamented 1.5 mm OD/0.86 mm ID (Sutter and World Precision Instruments) borosilicate glass on a P-97 Flaming-Brown puller (Sutter) using standard previously-described techniques[47]. The micropipettes were held in appropriately-sized holders complete with electrical and pressure connections (WPI). Electrical connections to the salt-solution were made using a silver wire exposed to bleach in order to generate a silver-chloride junction for effective continuity with minimal junction voltage and capacitance.

A pair of long-travel stages (ROBO-cylinders by Intelligent Actuator, IAI) carry the micropipette/ micromanipulator assembly and the well-plate/sample assembly. They are capable of movement at 300 mm/s with a resolution of 10 μm.

A Dell Precision Workstation running Windows XP forms the core of the system's control. A NI-6259 DAQ card (National Instruments), complete with four analog outputs, sixteen analog inputs, and 64 digital input and outputs was used for interfacing computer commands with the majority of the equipment. USB and serial ports were used for controlling Sutter equipment and IAI long-travel stages, respectively. Header files and interfacing code, written in C, were developed for the system. Details on their availability are discussed in Appendix C.

The voltage signal for electroporation is amplified using a high-voltage amplifier (Trek, Inc.), although for low-voltage tests (< |10 V|), the signal was derived directly from DAQ cards. A 100 kΩ resistor, a negligible value for the system, is placed in series with the electroporation circuit, and the voltage across it is recorded by the DAQ card. This value is then used to keep track of the current applied in the system.

4.2 Software Design

The entire automated SCE system is controlled through software written at the high level in MATLAB. The primary program, known as "Screen Control", used during operation of the system is shown in Figure 5 below and is detailed in the caption. Due to the fragility of many of elements of the system, the software keeps track of the position of all mobile components in addition to a select-set of fixed-position components in order to ensure no collisions or damage occur. Additional GUIs (not shown) enable shutter and exposure control of cameras as well as two-photon imaging and laser targeting if laser surgery is ever desired.

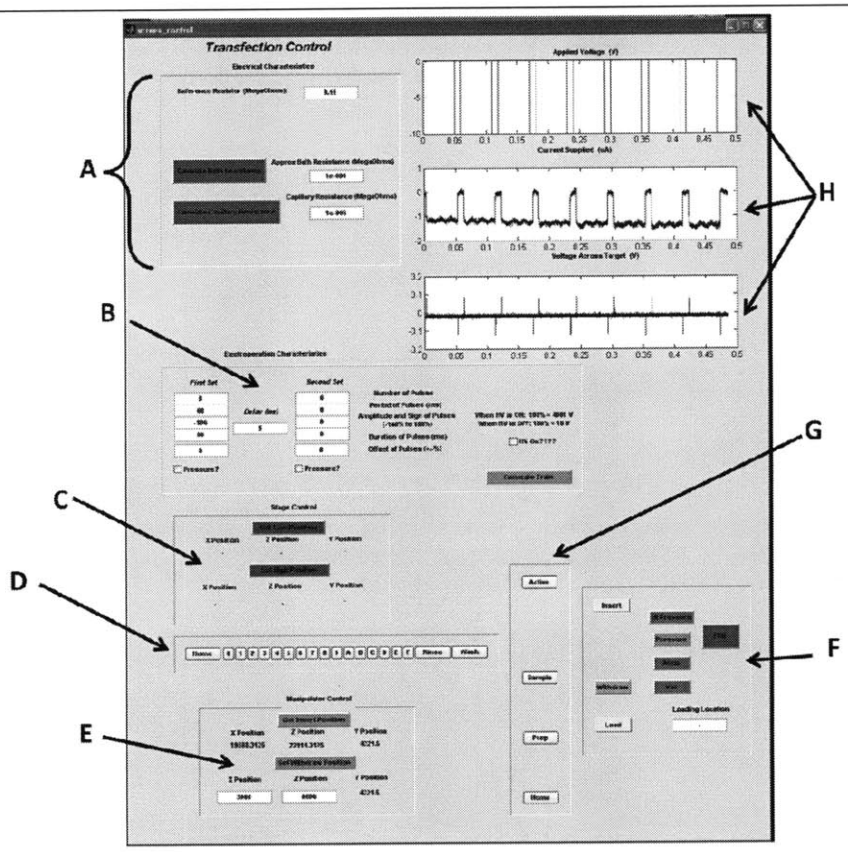

Figure 5| Screenshot of the GUI for "Screen Control", which controls most operations of the automated SCE system presented in this paper. Micropipette electrical characteristics, including resistance can be calculated in section **A**. The parameters of the electroporation pulse train are set by the user in **B**. Default stage positions can be set in **C**. Section **D** allows the user to select and keep track of the position of the sample tray and micropipette cleaning equipment. Micropipette positioning is entered and displayed in section **E**. Micropipette position, as well as pressure regulation, and electroporation triggering is controlled by section **F**. Section **G** allows the user to control and track the position of the micromanipulator/micropipette assembly position. The electrical data including applied voltage and recorded current as well as calculated voltage across the cell is displayed in the plots in Section **H.**

4.3 Overview of System Operation

An overview of the system operation is shown in Figure 6. First, the micropipette filled with conductive salt solution samples a particular agent by drawing in a pre-defined amount (A). Next, the sample well-plates are withdrawn, and the micropipette is moved to the tissue culture chamber and brought into the plane-of-focus of the microscope objective (B). The stage is brought into focus and a cell is targeted by the micropipette, at which point transfection takes place (C). This is repeated as many times as desired by moving the tissue culture to new locations, bringing the cell of interest in proximity to the micropipette, and triggering the electroporating pulse train (D). When finished, the micropipette is withdrawn from the slice bath and moved back to the loading stage where a cleaning bath is moved in. The tip is inserted into the bath and cleaned/rinsed (E) before sampling a new compound and repeating (A).

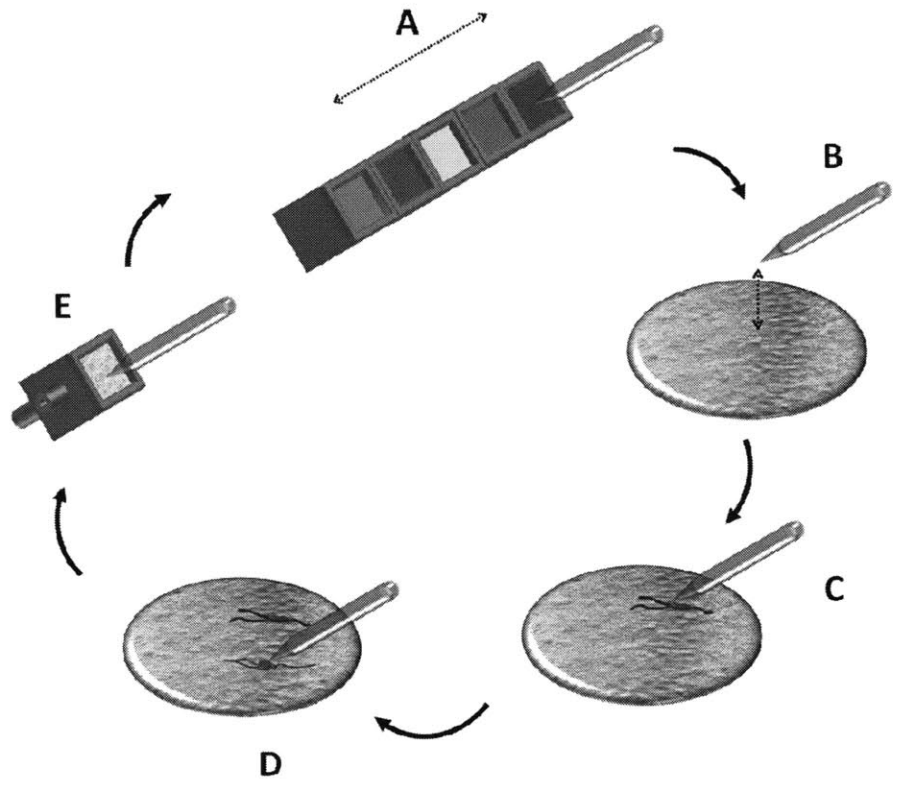

Figure 6| High-level overview of system operation presented in this paper. **(A):** A micropipette utilized as a large-bore low-hydraulic resistance microelectrode samples a labeling agent (fluorescent-protein encoding plasmid, Alexa Fluor™, etc...) from a solution holder. **(B):** The microelectrode is then placed into a known-position. **(C)**: The tissue is raised into the field-of-view and manipulated so that the tip can electroporate a region or single cell. **(D):** This procedure can be repeated for multiple cells if the same labeling agent is required. **(E):** Withdrawing the tip and then washing in either water, a bleach solution, or a pluronic acid bath, can then prep the tip for sampling another labeling agent while minimizing cross-contamination. The process can then be repeated multiple times at high speeds due to computer control and automation.

4.4 Stationary Micropipette and Mobile Sample

A significantly novel improvement to SCE presented in this thesis is the utilization of a fixed micropipette position and mobile stage, which is detailed in Figure 7 below. While in all past publications the micropipette itself has approached the sample for SCE, in the system presented, the micropipette always returns to a fixed position in the focal plane of the objective and the stage moves the tissue sample into and out of the plane of focus and in the x and y directions for easy targeting and alignment. Operating the system in this manner minimizes the risk of damaging the micropipette, and computer assistance allows the user to pre-target and store in memory cell locations to transfect before inserting the micropipette into the system in order to ease navigation during operation.

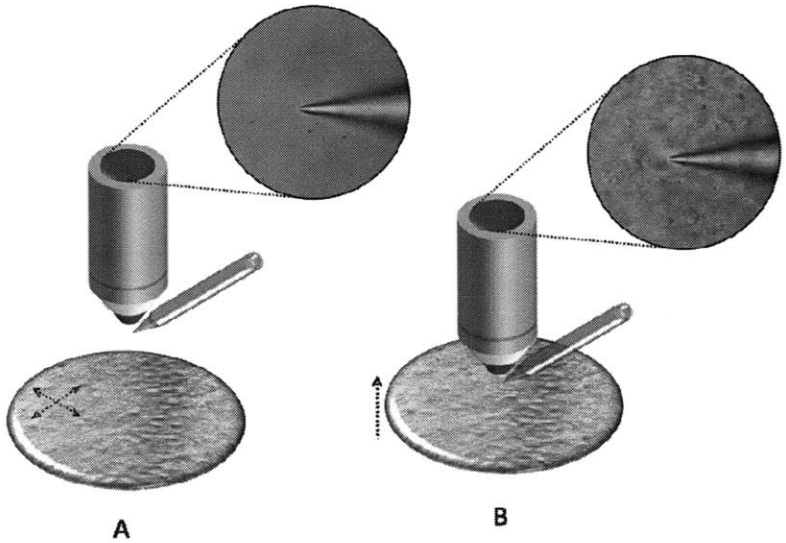

Figure 7| Stationary Micropipette and Mobile Sample Setup. The micropipette always returns to the same location in the field of view minimizing the risk of damaging it. The tip is inserted into the slice bath, when the tissue sample is below the focal plane **(A)**. At this point the tissue sample can also be moved around for targeting. When ready to electroporate, the sample is tissue sample is raised up into the focal plane such that the cell of interest comes into proximity with the SCE micropipette **(B)**.

4.5 Long Travel Stages and Micromanipulators

Placement of the micropipette, with its tip size of several microns, requires extremely accurate equipment and proper control. For the system to operate successfully, the micropipette must be quickly extracted and removed as well as cleaned and reloaded, all with a high degree of accuracy. The long-travel stages (IAI) and MP-285 micromanipulators (Sutter) are the equipment responsible for obtaining this accuracy. The long-travel stages have a reported resolution of 10 μm, which was found to be approximately correct in practice. The MP-285 micromanipulators generally have a reported repeatability of 1 to 2 μm, however by moving only along well-defined paths, backlash can be avoided, and the author found that this could be minimized to below 1 μm in some cases. Details are shown in Figure 8 below.

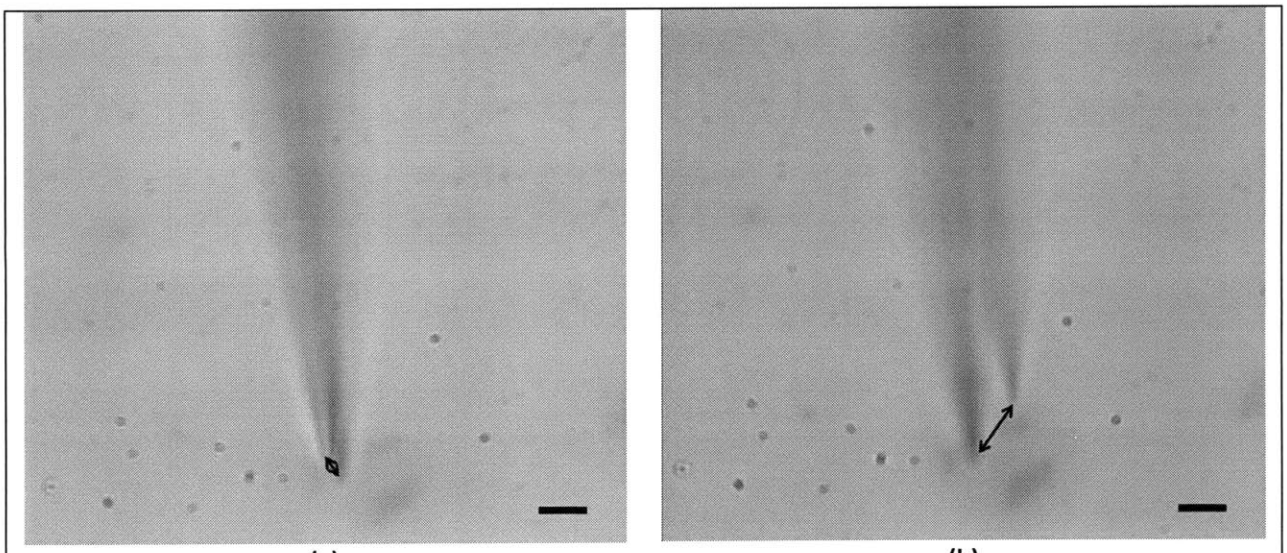

(a) (b)

Figure 8| The repeateability of the micropipette placement is depicted in the super-imposed before-and-after image sets above. **(a)**: The Sutter micromanipulator utilized has a published resolution of 0.120 μm and a repeatability of 1-2 μm, and this is approximately what is observed upon retraction and insertion into the fluid bath. **(b):** During a full cycle of operation where the micropipette is removed, the entire micromanipulator is moved backwards on the long-travel stage for loading or transfering of capillary contents, and then returned to its original start position, the 3-dimensional repeatability, $\Delta\rho$, has an average value of approximatley 10 μm. (Scale bar = 10 μm.)

On each cycle the absolute physical displacement of the micropipette tip, $\Delta\rho$, defined by (1) below, for a complete insert/removal cycle is measured at $\approx$ 10 um.

$$\Delta\rho = \sqrt{\Delta x^2 + \Delta y^2 + \Delta z^2} \tag{1}$$

By periodically resetting the long-travel stage (using its "HOME" function), and by fine-tune adjusting the tip position via the MP-285 by eye on each cycle of operation, a process which takes the user several seconds at most, the system can be made to have the ability to repeatedly cycle through full operation a large amount of times with little error. In one trial, the author was able to operate for thirty full cycles over the course of an hour with no problems whatsoever.

4.6 Pipette Loading and Cleaning and Diffusion-Limited Sampling

As mentioned above, the system utilizes a single micropipette as a reusable sample deposition and transfecting implement. In standard neurobiology, this is actually a rather novel approach to using micropipettes since it is generally common practice to back-load micropipettes with several μL of the agent of interest using a fine gauge syringe and then dispose of the micropipette when a new agent or sample is desired. The reusability of the micropipette stems from front-loading of the micropipette. Protocols for front-loading, do exist in cases of materials which are possessed in low quantities[20], however, these have exclusively been used for microinjection, not single-cell electroporation as we propose here.

At first glance, the fact that an electrical connection must be maintained with the loaded sample seems to forbid the use of front-loading with a conducting salt-bridge, since one would think that the salt-solution and the loaded sample would mix and dilute. However, such a conclusion is only valid at the macro scale, and at the scale of the micropipette geometries used for SCE, diffusion becomes a significantly slow process. This condition exists because the cross-sectional region across which diffusion occurs, shown as A in Figure 9 below, is extremely small, being in the range of 100's of microns.

For the volumes we plan to use in the system, a supercoiled plasmid, in a patch pipette will maintain an approximately constant concentration at the tip for up to fifteen minutes or more based on calculations and verified by imaging SYBR Green-labeled plasmid presence in the tip of micropipettes. To the knowledge of the author this is the first attempt of its kind to merge front-loaded sampling with SCE, and experiments thus far have confirmed that it is possible.

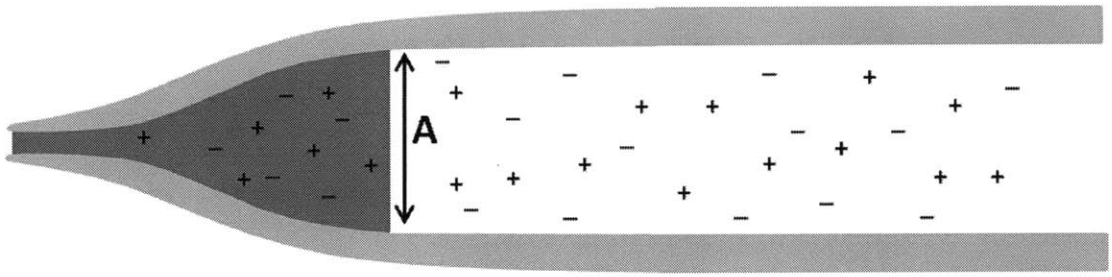

Figure 9| The diffusion rate of the loaded sample (shaded/blue region) is directly proportional to the cross-sectional area of the micropipette (A). A universal standard salt solution (white region) maintains electrical contact with the loaded sample. Depending on micropipette geometry, diffusion coefficient of the molecule of interest, and volume loaded, the concentration of loaded sample at the tip can be maintained at relatively stable levels for up to fifteen minutes in the case of supercoiled plasmids used in this paper.

For cleaning of the micropipette, a variety of chemicals were considered and tested, however the most successful for cleaning and minimizing cross-contamination between sampling was found to be a simple 50/50 mixture of sodium hypochlorite (bleach) and water. By first ejecting any left-over transfection agent, and then quickly drawing in and then ejecting cleaning solution for approximately five seconds, followed by several rinses in de-ionized water, even traditionally "sticky" materials such as plasmids can be effectively cleared.

4.7 Pressure and Vacuum Control

For loading and rinsing, as well as depositing the transfection agents, a pressure system was constructed as shown in Figure 10. It is computer-controlled through the DAQ card, and in its current realization provides two different positive pressures (high gauge pressure of 35 mbar to 2000 mbar and a low gauge pressure of 0 to 35 mbar), one negative pressure (-35 mbar to 2000 mbar), and a zero gauge pressure (atmosphere). The system software keeps track of how long each pressure is applied through the micropipette, as well as the applied pressures and can use these numbers to roughly calculate durations needed for loading and cleaning tips. In addition, the basic setup is expandable for future improvement.

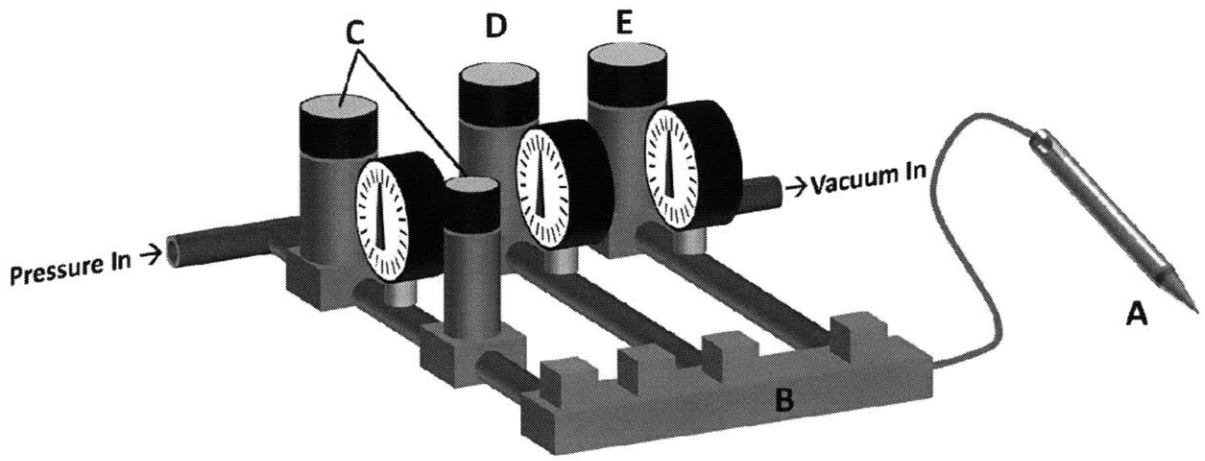

Figure 10| The pressure applied to the micropipette **(A)** is selected by a computer-controlled valve bank **(B)**. For the system version utilized in this thesis, four different gauge pressures are generally used: Atmospheric pressure, a low positive pressure generally in the range of 0 to +50 mbar which is fine-controlled by the rough regulator and trimmer regulator **(C)** a high-pressure for cleaning and loading at approximately +35 to 2,000 mbar **(D)**, and vacuum at approximately -2000 mbar **(E)**. Tubing is trimmed to minimum lengths, and where possible, non-expanding tubing is used to minimize response time of the system to pressure changes.

4.8 Micropipette Approach Angle and Tissue Contact Minimization

A steep approach angle is a common desire in neurophysiology, particularly for patch clamping and SCE in tissue culture. This is because of the fact that such techniques require micropipettes with shorter tapers which can therefore cause more tissue damage at shallower approach angles as shown in Figure 11. In the case of an inverted microscope where the objective is below the sample and the condenser is generally several centimeters above the sample, very steep micropipette approach angles are obtainable because nothing is in the way. Inverted microscopes, however are only effective in imaging dissociated cells, single cell layers such as keratinocytes cultures, or extremely thing tissue culture. Thicker tissue culture, such as organotypic slices, prevent inverted imaging of an inserted micropipette (done from the upright side) because of light scattering through the tissue. Consequently, in tissue culture work it is very common to use an objective lens which is on the same side as the micropipette. More often than not these objectives are water immersion which permits a greater numerical aperture (NA) and working distance, however the presence of the objective on the upright side of the slice imposes a more stringent limitation on the approach angle as highlighted in Figure 12.

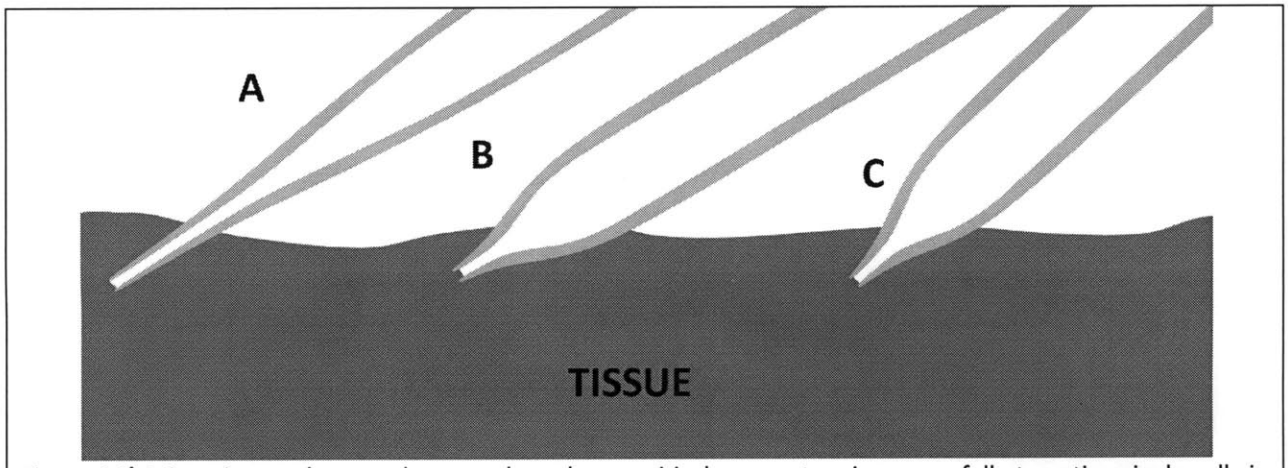

Figure 11| Micropipette shape and approach angle are critical parameters in successfully targeting single cells in tissue with minimal damage. While for micropipettes with narrow geometries **(A)**, deep penetration at shallow angles can be made with minimal collateral contact, the relatively high-resistance of the pipettes (>20MΩ) impairs its effective application to rapidly front-loaded single-cell electroporation as highlighted in sections above. Micropipettes with geometries closer to patch clamp pipettes suitable for SCE described in this paper make significantly more collateral contact with tissue culture at shallow approach angles **(B)**, but this can be minimized by approaching at a steeper angle to the horizontal **(C)**.

The discovery and explosion in popularity of patch clamping in the early 1980s, led all the major microscope manufacturers (Nikon, Olympus, Zeiss, and Leica) to develop sets of extremely versatile water immersion objectives with large working distances and large numerical apertures. Recent years have seen the appearance of so-called "workhorse" objectives which often possess a magnification in the range of 16× to 20× and consequently a large field of view as well as an NA in the neighborhood of 0.8 to 1.0, and a working distance of about 2.0mm to 3.0mm. These objectives are often utilized in conjunction with magnification-changing head units on microscopes to allow one to change the net magnification observed by the researcher without necessitating a change of objective which can disturb the sample as is obviously the case of water-immersion objectives.

The front-loading requirement on the micropipettes requires a short micropipette taper on par with that of traditional patch pipettes, and consequently one will want to approach at a steep approach angle if possible. An analysis of the physical limitations of water immersion electrophysiology objectives on micropipette approach angles follows.

4.9 Limitations from Water Immersion Objectives

When advertising water immersion objectives, the four major manufacturers of microscope optics always make a point to emphasize the nose taper of the objective. However, the author investigated these taper angles and found that standard microcapillary pipettes can often times not take advantage of the full taper angle. Shown in Table 1 below is a list of water immersion electrophysiology objectives from four major manufacturers, along with details important for approach angle calculations

By using relatively simple geometries, one is able to generate an equation for how far into the field of view a short-tapered pipette will be able to "penetrate" for a given objective. Shown in

Figure 12 and Equation 2 a micropipette with an outer radius of w_{or} approaching at an angle of θ to the horizontal the nose piece of an objective lens with working distance w_d field of view radius f_r, and nose diameter n_r will penetrate a distance d_v into the field of view.

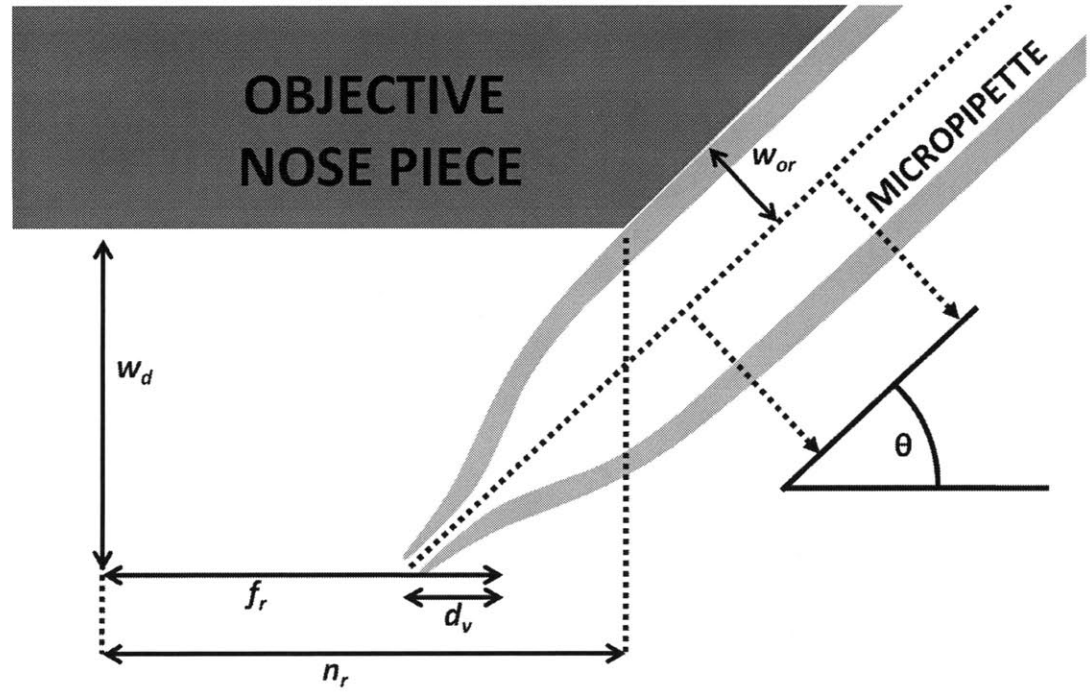

Figure 12| Diagram of pipette approach angle and the physical restrictions which it imparts on the system.

$$d_v = \frac{w_d}{\tan(\theta)} - \frac{w_{or}}{\sin(\theta)} - n_r + f_r \tag{2}$$

It is interesting to note that in applying these equations it becomes apparent that the steep tapers, which are often heavily advertised in selling the objectives are not useful with the standard range of pipette glass (1.0 mm to 1.5 mm outer diameter). For example in Table 1, note that while the Olympus 10X objective has nose taper of 50°, the small field of view and relatively larger nose diameter prevent any glass greater than 0.8 mm in diameter (rarely used in electrophysiology) from actually taking advantage of the full 50° of approach room provided

A total of six objective lenses were analyzed using Equation 2 and three were tested. All three tested objectives possessed similar FOV penetration depths to what was calculated. What can be drawn from this study is that while several companies produce objectives which do enable steep approach angles, many advertise approach angles as the nose-taper angle, which is incorrect since the finite diameter of the micropipette glass limits and can even prevent the field-of-view penetration of standard sized pipettes in some cases, as described in the derived equation above. In fact, the only objective analyzed that could fully use its nose taper angle with 1.0 mm O.D. glass was the Nikon 16× 0.8 NA objective, which is consequently the objective used in constructing the system presented in this paper.

As a brief aside, during the course of work the author discovered that the well-known lack of symmetry in the taper angle of many pulled-glass micropipette geometries can be used to improve FOV penetration depth by up to 25% by carefully selecting the rotation orientation of the glass in its holder so that the microscope objective comes in contact with the more shallow-tapered side.

Objective	W.D. (mm)	Nose Taper Angle	Nose diameter (mm)	Field of View (mm)	Ma FOV Penetration θ with 1.0 mm OD Glass
Nikon 16X 0.8 NA*	3.0	45°	6.0	2.0	45°
Zeiss 20X 1.0 NA†	2.0	38°	4.7	1.0	36°
Zeiss 40X 1.0 NA†	2.5	37.5°	6.6	0.5	32°
Zeiss 63X 1.0 NA†	2.123	37°	5.82	0.32	30.2°
Olympus 20 X 1.0 NA*	2.0	38°	5.24	1.1	34°
Olympus 20X 0.5 NA*	3.5	55°	5.3	1.325	53°

Table 1| A compiled list of the true maximum taper angles for various water-immersion objectives made by three of the four major manufacturers. Note: Values marked with an * were physically measured and calculated by the author due to restrictions on available engineering drawings. Values marked with a † used numbers taken from publicly available literature provided by the company for calculations.

5. Electroporation and Delivery of Transfection Agents from Micropipettes

A layer of complexity in analyzing single-cell electroporation surfaces when one considers the fact that the electrical signal itself serves not only as the means of opening the cellular membrane, but also, under certain conditions, can be the key motive force acting on the agents to be transfected. Consequently, the characteristics of the electrical signal must not only be of satisfactory for porating the cellular membrane but also to effectively move the agents to be transfected into close proximity with the cell membrane or into the cell.

There has been relatively little work done in the study of the movement of molecular species at the tip of the micropipette, with a few notable exceptions[43, 44]. It is recommended in several SCE papers[36, 39] that hyperpolarizing (negative) pulses should be used for delivery of negatively charged labeling agents or plasmids. The justification for this is that the negative charge of the transfection agent is repelled from the negative electrical potential inside the pipette causing it to exit the tip. The negative charge, of course, arises from the fact that the phosphate backbone of the double-helix of DNA is highly-deprotonated at a standard physiological pH of 7.4[48].

This charge-repelling motion is not the whole case, however, for because the micropipettes used are made of glass, electroosmotic flow also exists, and in the case of hyperpolarizing pulses, the direction of this flow is *into* the pipette; in other words it directly opposes the charge repelling flow, termed electrophoretic flow. Additionally, in the case of SCE in tissue culture and *in vivo* conditions, applying a positive pressure of a few to several dozen mbar is necessary to avoid clogging and this further influences the delivery of the transfection agents.

5.1 Analysis of the Three Competing Forces

Electroosmotic flow is governed by the following equation

$$u_o = E\mu_o \tag{3}$$

where u_o is the electrosmotic velocity, E is the electric field, and μ_o is the electroosmotic mobility which is defined as:

$$\mu_o = -\frac{\epsilon\zeta_{glass}}{\eta} \tag{4}$$

where ϵ is the relative permittivity of the buffer media (F/m), ζ_{glass} is the zeta-potential of the borosilicate glass wall, and η is the dynamic viscosity. For borosilicate glass ionization of SiOH molecules result in a fixed native negative charge present on the surface of the capillary which gives a native negative value for ζ_{glass}, however in practice ζ_{glass} may be a wide range of values including positive, negative, and zero depending on pH and ion concentration of the buffer[49-51]. In standard physiological conditions (total ion concentration ~ 0.3 M, pH ~ 7.4), glass has a ζ_{glass} ≈-20 mV. This results in a $\mu_o = -1.4 \times 10^{-4}$ $cm^2 \cdot V^{-1} \cdot s^{-1}$. An important, well-known conclusion from this value is that at standard electrophysiological conditions, electroosmotic flow moves from anode to cathode[52-55]. In other words, during a hyperpolarizing pulse in SCE, electroosmotic flow is into the tip of the capillary.

The existence and direction of this flow was confirmed by imaging the shockwaves generated from a micropipette containing physiological salt solution placed in brain tissue. When positive pulses were applied, an outwardly expanding compression wave was visible in the tissue, indicative of an outward flow from the tip. When negative pulses were applied, the tissue was drawn towards and even into the micropipette tip, indicative of flow *into* the tip.

In the case of electrophoretic flow, direction of movement is based upon the charge of the mobile species, not the charges existing on the wall of the channel as is the case with electroosmotic flow. Electrophoretic flow is governed by Equation 5,

$$u_p = E\mu_p \tag{5}$$

where u_p is the electrosmotic velocity, E is the electric field, and μ_p is the electroosmotic mobility which for small molecules is described as

$$\mu_p = \frac{Dqz}{kT} \tag{6}$$

where D is the diffusion coefficient, q is the unit charge of an electron, z is the integer charge of the molecule, k is Boltzman's Constant, and T is temperature. In the case of micropipettes, if a negatively-charged species is present, the electrophoretic flow will be *into* the micropipette during positive pulses (opposites attract), and *out of* the micropipette during negative pulses (like repels like).

The third motive force at work inside the micropipettes is from applied pressure. Generally the pulled glass micropipettes possess significant hydraulic resistance due to the relatively small opening at the tip, which is on the order of several μm. For a circular channel, hydraulic resistance over a short cylindrical channel of constant radius is described by Equation 7 below, where η is dynamic viscosity, L is the length of the channel segment under consideration and r is the radius of the channel.

$$R_{hyd} = \frac{8\eta L}{\pi r^4} \tag{7}$$

While the changing channel radius of the micropipettes used for SCE prevents directly applying Equation 7 for finding hydraulic resistance, it still reveals a fundamental phenomenon in the system: because the hydraulic resistance scales to the inverse of the channel radius to the fourth power, almost all hydraulic resistance is seen in the tip of the micropipette.

When electroosmotic, electrophoretic, and pressure-driven flows are considered together, Equation 8 is developed. The velocity of a given particle at a given point in the micropipette with internal radius r is based upon this equation.

$$u_{tot} = \frac{P}{R_{hyd}\pi r^2} + E(\mu_p + \mu_o) \tag{8}$$

In most cases of SCE, the pressure-driven flow is kept low enough that we need only to consider the simplified Equation 9, however.

$$u_{tot} = E(\mu_p + \mu_o) \tag{9}$$

Equation 9 was investigated by loading the relatively low-molecular weight fluorescent labeling agent Alexa Fluor 594 hydrazide (Invitrogen), also called AF594, in physiological salt solution in the tip of a micropipette. The molecule, depicted in Figure 13, has a molecular weight of 894 Daltons, and a pKa of 7.2 due to the pair of R-SO_3 groups on the molecule. Importantly for the sake of this experiment, this pKa is exceedingly close to the standard pH of most physiological solutions such as EBSS or PBS (pH~7.4), so by altering the pH above and below this pKa, one should be able to manipulate the effective charge of the AF594 molecule which flows are dominating.

Alexa Fluor 594 has a diffusion coefficient ranging from 2.4×10^{-6} $cm^2\cdot s^{-1}$ to 3.7×10^{-6} $cm^2\cdot s^{-1}$ depending on whether one is water or cytoplasm[56]. As a result, when sufficiently above its pKa of 7.2 (with both of its SO_3 deprotonated), $\mu_{pAF594} = 2.9 \times 10^{-4}$ $cm^2\cdot V^{-1}\cdot s^{-1}$. However, normal physiological pH to which most material is buffered is 7.4, and in practice it can be lower than this, particularly due to the electrolysis occurring if an anode is present. Consequently, the z is rarely 2 at pH of 7.4. In fact, it will be closer to 1.2 to account for significant protonation, and consequently $\mu_{pAF594} = 1.8 \times 10^{-4}$ $cm^2\cdot V^{-1}\cdot s^{-1}$. At a pH of 5.9, significantly below its pKa, the molecule is protonated to the point where we can assume $\mu_{pAF594} \approx 0$ $cm^2\cdot V^{-1}\cdot s^{-1}$. Throughout

this range of pH values, the electroosmotic mobility should remain approximately constant at $\mu_o = -1.4 \times 10^{-4}$ cm^2·V^{-1}·s^{-1} based off of a ζ_{glass} ≈-20 mV.

As shown in Table 2 below, at high pH values, where AF594 was fully deprotonated, the molecule tends to move out of the tip of a micropipette firing hyperpolarizing pulses. This indicates that electrophoretic flow is dominating. Even at pH = 7.4, where AF594 hydrazide is only partially deprotonated, electrophoretic flow dominates, albeit the observed flow rate is less significant indicating that the two forces are closer to being balanced than at pH 7.8. At a low pH of 5.9 the AF594 is effectively fully protonated, and therefore carries little to no charge. The result of this is that the molecule now flows in the opposite direction to that which it did at a pH of 7.4 or 7.8, indicative of electroosmotic flow now being the dominant force.

pH	μ_{pAF594} (cm^2·V^{-1}·s^{-1})	μ_o (cm^2·V^{-1}·s^{-1})	Predicted Dominant Flow	Experimentally Determined Flow
7.8	2.9×10^{-4}	-1.4×10^{-4}	Electrophoretic	Electrophoretic
7.4	1.8×10^{-4}	-1.4×10^{-4}	Electrophoretic	Electrophoretic
5.9	≈ 0	-1.4×10^{-4}	Electroosmotic	Electroosmotic

Table 2| Electroosmotic and electrophoretic flows in Alexa Fluor 594 for different pH levels. The dominant flows for all three conditions were predicted and verified experimentally.

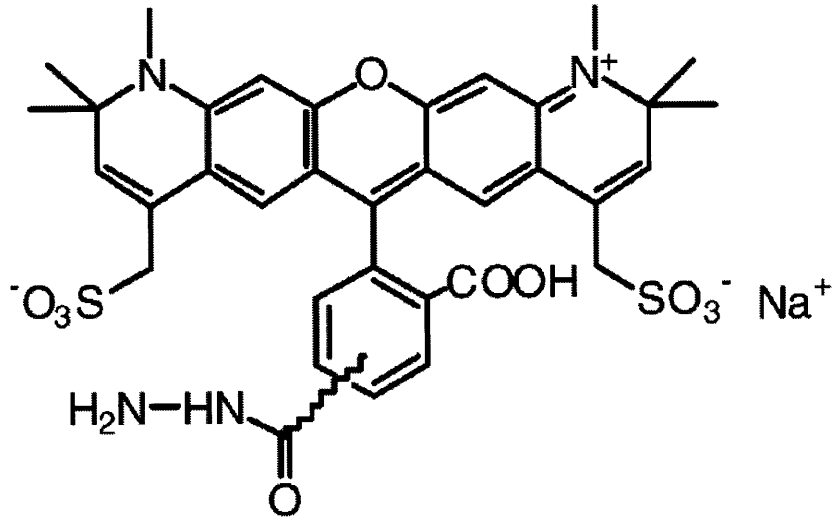

Figure 13| Molecular structure of Alexa Fluor 594 hydrazide salt. In solution, the negative charge of the dye is carried by the two R-SO_3 groups, which have a pKa of approximately 7.2, very close to physiological pH. For labeling purposes, it is therefore critical that pH is kept above this value. Generally this is done at pH 7.4.

5.2 The Question of DNA Transport in SCE

The analysis of Equation 9 via the study of Alexa Fluor 594 hydrazide, provides a good starting point for the study of plasmid movement during transfections. This is extremely important since long-term labeling in cultured slices is generally only obtainable by transfecting genetic material such as fluorophore-expressing plasmids.

Plasmids have rather low diffusion coefficients[57]. For a 4.7 kbp plasmid, it is on the order of 3.5 $\mu m^2 \cdot s^{-1}$, which is approximately 2 orders of magnitude less than that of Alexa Fluor 594. Additionally, the relatively large size of plasmids, even in supercoiled state generally prevents Equation 6 from being used reliably. Instead, the plasmid itself can be assigned a zeta potential ζ_{DNA} much as is the case for glass capillary walls in determining electroosmotic mobility. As a result, plasmid electrophoretic mobility is described by Equation 10.

$$\mu_p = \frac{\epsilon \zeta_{DNA}}{\eta} \tag{10}$$

Because of the negative charge present in the phosphate backbone of the plasmids, ζ_{DNA} is also negative. At physiological pH, ionic concentration, and temperature, ζ_{DNA} is approximately the same size as ζ_{glass}Error! Bookmark not defined. [26, 48, 53, 58]. This results in an interesting predicament because if the two values are approximately the same they will tend to partially or fully cancel out as indicated in Equations 4 and 9. While some researchers have forwarded arguments that one force does clearly dominate[44], the difference between ζ_{DNA} and ζ_{glass} will still be only a few mV at the most in standard physiological condition, and at this level, pressure controlled flow may in fact dominate in the SCE system presented in this paper. Several experiments conducted by the author do tend to support this idea, for in the case of AF594 studies at low applied pressures of 10 to 20 mbar, applying positive and negative signals on the order of magnitude of 10 V will significantly affect the direction and flow rate of the molecules in the manner expected (see previous section), however, when the same signals are applied to plasmids labeled with SYBR Green, little to no change is seen in the direction is visible. When the applied signals are increased to higher voltage, the plasmid movement tends to suggest electrophoretic dominance ($|\zeta_{DNA}| > |\zeta_{glass}|$) which agrees with several SCE publications[14, 36, 59]. Taking all of this into account, the evidence tends to suggest that both electrophoretic flow and pressure-driven flow are the dominant means of ejecting plasmids out of the tip of the micropipette during SCE.

5.3 "Invisible" Tip Clogging

As discussed in Figure 2 of this thesis, it is common practice to look for tip clogging in SCE by monitoring the current measured in the system. During the course of system development, an interesting phenomenon was discovered where the tip appeared clean under brightfield/IRDIC and looked electrically clean as well, but it turned out to not be releasing DNA. This was initially not detectable by the author, since the plasmid was unlabeled and therefore not capable of being visualized in real time. Inability to get plasmid expression was the only indicator of tip clogging, but this could not be determined until 24 hours post-transfection. Co-loading Alexa Fluor 594 with plasmid, initially revealed the electrically invisible tip clogging, and by adding the DNA stain SYBR Green to the transfection solution, the author was able to visualize in real-time the release and/or clogging of the micropipette tip by DNA.

Investigation into the causes of this clogging revealed that it was only slightly concentration dependent. The concentration of the plasmid in the sample solution was varied from 30 ng/μL up through 1.0 μg/μL and in all cases clogging of the tip by DNA was visualized. Additionally applying higher voltage pulse trains was found to more quickly elicit the clogging, and this

causes the author to suggest that a process similar to what is shown in Figure 14 may be taking place. Namely that under normal conditions the plasmids can easily flow out of the narrow tip, but due to the focusing nature of the inside of the micropipette tip at significantly high voltages, which cause significantly higher particle velocities, a "traffic jam" of sorts may develop which blocks the passage of further plasmids, but which can still allow smaller ions to flow into and out of the tip allowing for electrical continuity to remain as is seen experimentally.

This clogging phenomenon is currently under investigation as this thesis is written, but significant headway has been achieved by periodically cleaning micropipette with a 50/50 water/bleach solution. Doing so seems to minimize the buildup of plasmid at the tip which leads to clogging, however it does not fully eliminate it. Since this cleaning bath is already present and used in our system for cleaning between sampling, this does present one feasible means of getting around the problem. It will be desirable to completely solve this problem, however, in order to ultimately increase the efficiency of the system overall.

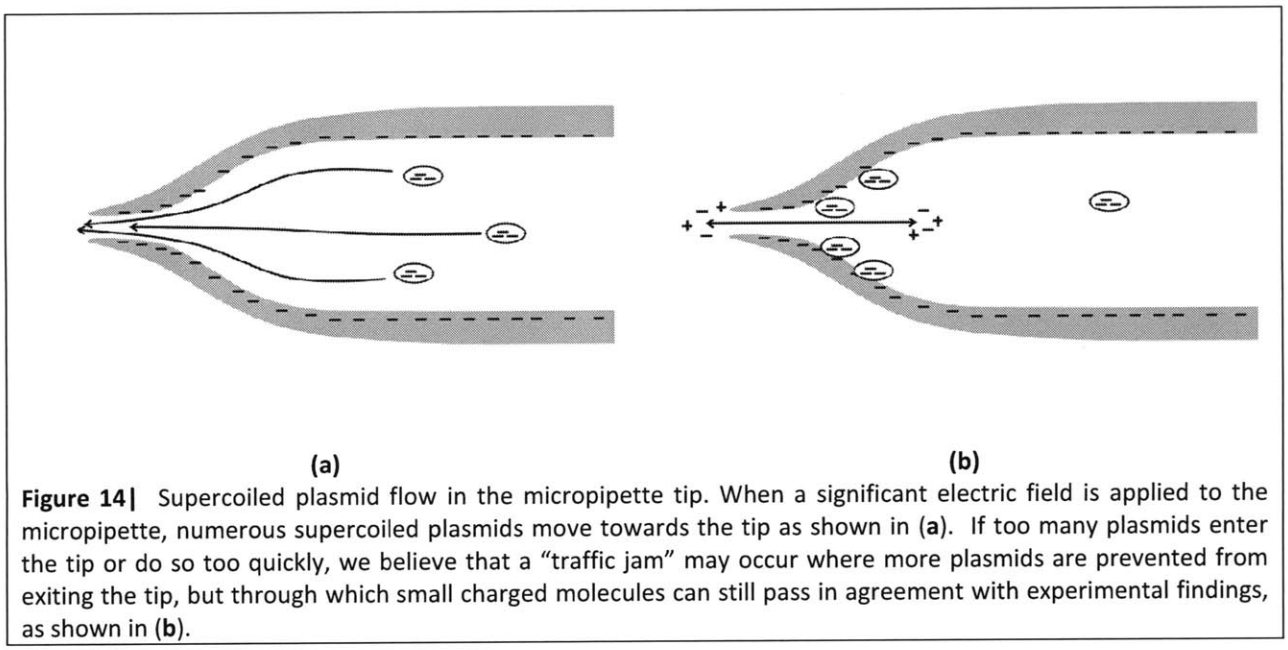

Figure 14| Supercoiled plasmid flow in the micropipette tip. When a significant electric field is applied to the micropipette, numerous supercoiled plasmids move towards the tip as shown in (**a**). If too many plasmids enter the tip or do so too quickly, we believe that a "traffic jam" may occur where more plasmids are prevented from exiting the tip, but through which small charged molecules can still pass in agreement with experimental findings, as shown in (**b**).

6. The Hippocampus as a Cultured Tissue Platform

All elements of this paper up until now have involved the technology used for transfecting of single cells in tissue culture, but not the tissue culture itself. The following section will remedy this situation. As mentioned in the text above, the region of neural tissue most commonly used in organotypic culture is the hippocampus, although other regions of the brain including the cortex have been utilized[30, 60]. Generally tissue is taken from standard wild-type rats (Sprague Dawley, Wistar, etc…). Mouse tissue may also be used, although the author and several other neuroscientists have found it more difficult to maintain than rat tissue. Additionally, there is the potential to use human tissue in organotypic culture platforms as has been investigated previously, although the work conducted so far is really only preliminary[61-63].

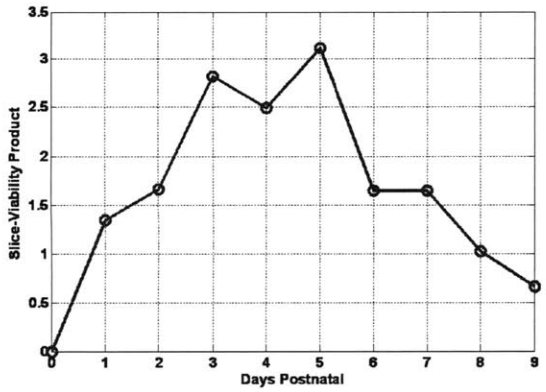

(a)

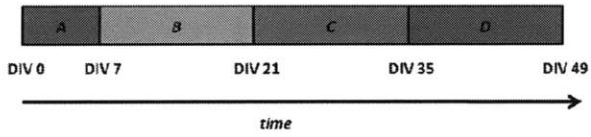

(b)

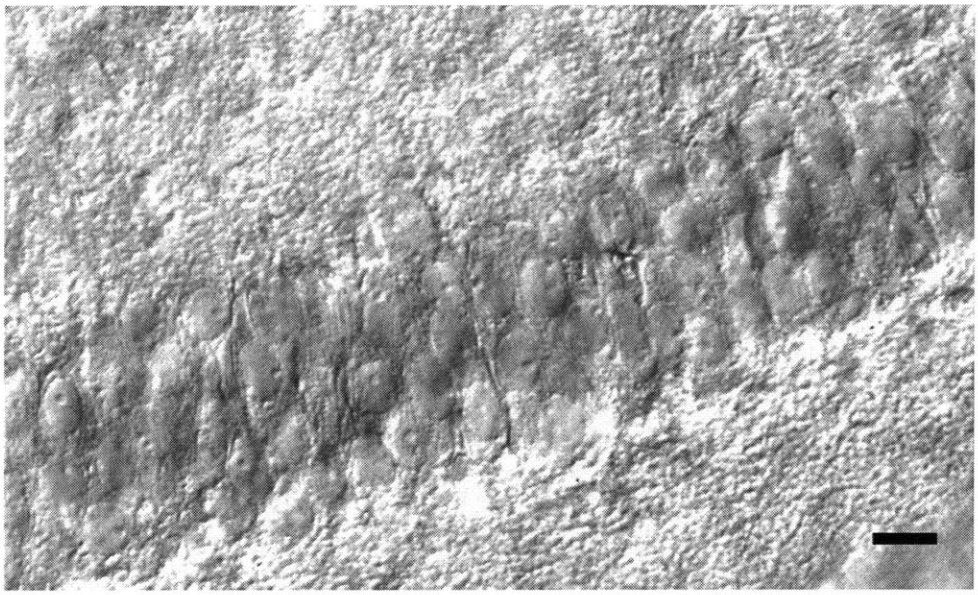

(c)

Figure 15| (a): Quantitative analysis of hippocampal slice viability and quantity as a function of organism age at point of harvest. Multiplying the average number of slices which can be collected from a rat pup of a certain age by the percentage of viable slices at DIV7 yields which shows the ideal age for tissue harvesting to be around P3 to P5. It was noticed that younger slices seem to stabilize quicker on the membrane, and consequntly most tissue was collected at P3 or P4. **(b):** Using the culture techniques described in this thesis, we have kept hippocampal slices in culture for at least 50 DIV, however, the architecture of the slice tends to begin breaking down at around the 35 DIV. For the seven days immediately following harvest and plating, no transfections are conducted in order to allow settling and thinning of the slice. By around 7 DIV, the pyramidal cell layer and granule cells will be relatively stabilized and approachable to micropipettes. For the next two weeks until 21 DIV, transfections can be carried out on the cells with relative ease. After 21 DIV, we no longer carry out transfections due to an increase in the changes of the slice, although imaging is still very easy and the tissue is valid for imaging and screening studies. At around 35 DIV, the pyramidal cell layer will begin to dissociate, and the tissue will become more difficult to work with both as a model of study and from technical perspectives. **(c):** CA1 pyramidal cells at 7 DIV in an organotypic hippocampus slice taken from a P4 rat pup. Note the clearly defined edges of the cell soma, indicative of viable, structurally competent cells, and the nuclei visible as the small round shapes. Scale bar = 10 μm.

Tissue is collected generally during the first 10 days following the birth of rat pups. While there are numerous protocols which report on a vast array of ages and success rates for tissue, using the media described in Appendix A, we found an ideal age of harvest based at about P3 to P5. This is due to the fact that the older the pup at the time of harvest, the more slices which can be collected, but at the same time as the pup ages, it becomes both harder to successfully harvest the slices and harder to culture them to a mature functional state. In taking culture results from several months (approximately 24 slice setting sessions), when the number of slices and viability percentage are multiplied together for different ages, the plot shown in Figure 15(a) is generated, revealing that P3 to P5 provide the most effective time of harvest. Once plated, the slices must be allowed to settle and acclimate for approximately seven days. Further restrictions on usage are roughly outlined in Figure 15(b) above. For our usage, a clean, well-defined CA1 pyramidal cell layer is needed, which should ideally resemble that which is shown in Figure 15(c) at 7 DIV.

7. RESULTS

The system presented in this paper is still in the process of being refined, however basic processes fundamental to successful operation have all been performed and are demonstrated below.

7.1 Alexa Fluor Transfection Efficiency

Neurons in the CA1 to CA3 region of the hippocampal cultures were transfected with Alexa Fluor 594 hydrazide (Invitrogen) at a concentration of 500 μM. The micropipettes used had electrical resistances of approximately 10 MΩ, and the transfection signal applied was -20V at 200 Hz and 20% duty cycle for 1 second. Within seconds of transfection, the dye was visible far into the processes of the cells. As shown in Table 3 below, 100 cells were targeted, and a very high percentage, 97%, showed some form of expression immediately following transfection. At 24 hours post-transfection, the cells were imaged again, and approximately 83% of cells were found to still possess concentrated AF594. At 48 hours post-transfection this number dropped slightly to 78% of cells. These values are comparable to those found in the literature[38].

Time (hours post-transfection)	Survival Percentage
0	97%
24	83%
48	78%

Table 3| SCE and survival rates of AF594 into a set of CA1 and CA3 pyramidal cells in an organotypic hippocampal tissue culture (n = 100).

7.2 Successful SCE of Plasmids

At the time of writing we are still working on perfecting the successful SCE of plasmids into cells into tissue culture. While previous researchers have demonstrated plasmid transfection efficiencies of as high as 80 to 90%[14, 36, 43] we have struggled to match this value often times obtaining transfection efficiencies peaking at 25%. Currently we believe the decreased efficiency is due to tip clogging, discussed in Section 5.3 above. Consequently, full system operation has

not been carried out yet, although the individual pieces have been demonstrated at almost full functionality. Figure 16 below shows successful SCE transfection obtained by our system of two different types of fluorophore-encoding plasmid into pyramidal cells in organotypic tissue cultures. Additionally, four types of plasmids have been successfully transfected into tissue slices using the system presented in this paper, including a tdTomato encoding plasmid driven by an HSV promoter as well as a trio of plasmids based off of Clontech's pEGFP-N1 plasmid, one of which encodes mRFP, and one of which encodes YFP.

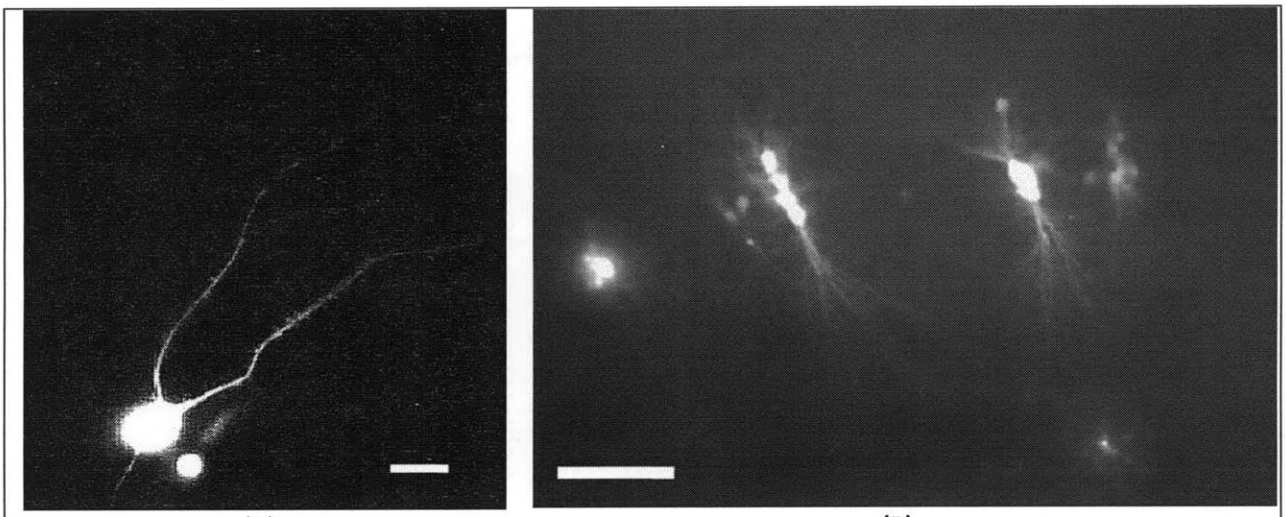

(A) (B)

Figure 16| Two images of cells electroporated with plasmids. Image **A** is a CA3 pyramidal cell transfected with a plasmid expressing tdTomato driven by an HSV promoter. Note the visibility of spines on the dendrites (scale bar = 10 μm). Image **B** is a set of CA1 pyramidal cells transfected with a pEGFP-N1 plasmid (scale bar = 100 μm). Ultimately the goal of this research is to have multiple agents expressing in the same slice

7.3 Sampling and Deposition

A core portion of the system functionality is the ability to flawlessly insert, transfect, withdraw, clean, and sample using the micropipette without causing damage to the tip. Time-trials and full-cycle robustness trials were carried out on the system. A full operation cycle, similar to that illustrated in Figure 6 was found to be obtainable in approximately 60 to 90 seconds depending n the amount of time spent cleaning the micropipette. Additionally, full-cycle operation was repeated thirty times (approximately one hour in duration) using the same micropipette with very little positional drift and no catastrophic collisions which damaged the tip beyond functionality. These tests were carried out using physiological salt solution, however, and work using plasmids must still be done.

Because of the high diffusion coefficient of Alexa Fluor dyes, it is difficult to use a collection of them for sampling and transfection in slice. Plasmids, having diffusion coefficients approximately two order of magnitude less, can be much more reliably used with the system presented, however due to clogging issues discussed in above sections, we cannot yet use them in testing the full functionality of the system. As a result, in order to test the sampling and deposition elements of the system a series of colored dyes were samples using the system and

deposited by the micropipettes onto parafilm, as shown in Figure 17 below. The full deposition was carried out in roughly seven minutes.

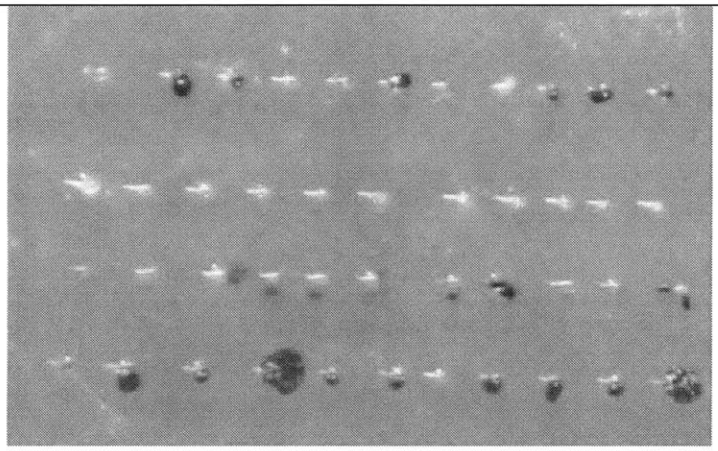

Figure 17| Early proof of concept demonstration of system loading and depositing technique. Placement of small drops of colored dye from standard low-resistance patch pipette done on parafilm in a non-water filled dish. Total deposition time from start to finish took seven minutes. (40X)

8. CONCLUSION

Organotypic tissue slice cultures provide a convenient middle ground for the study of neuronal populations, possessing many of the characteristics of a true *in vivo* system while at the same time providing the convenient imaging and ease of accessibility found with *in vitro* systems. Current manipulation techniques, many of which are low-throughput in nature, are incapable of effecting the full potential of organotypic cultures, however. Consequently a technique which allows the reliable and rapid transfection of different compounds such as labeling markers into subpopulations of cells inside a single tissue culture slice would be extremely useful, permitting easy study and imaging of sub-cellular features, axonal and dendritic dynamics, and even cellular migration in real time.

Introducing multiple, distinguishable labeling agents via single cell electroporation, as proposed and presented in this thesis, allows cellular characteristics to be studied at higher densities, and is thus a more efficient use of organotypic tissue. In some situations, it is also an inherently simpler, more cost effective, and less time-consuming solution for labeling than development of transgenic lines. At the same time, however, it provides single-cell selectivity, something which viral transfections generally do not guarantee.

The high efficiency and high-density labeling yielded by the presented design could additionally open the door for use of other tissue types traditionally not commonly used for organotypic slice culture. For example human neural tissue from post-mortem and fetal sources has been cultured to some success in previous work[61-67]. Such tissue is quite rare, and it is therefore necessary to efficiently utilize it. Overall however, the automated SCE system presented will allow for greater utilization of cultured tissue and the improvement of its status and ability as a biological platform to provide meaningful results in an efficient manner.

LIST OF FIGURES

BIOGRAPHICAL NOTE

Joseph Steinmeyer graduated from the University of Michigan, Ann Arbor in 2008 with a B.S.E. in Electrical Engineering. While there he conducted biomimetic research on harvesting evaporative energy using designs inspired by structures found in plant leaves for the Maharbiz Research Group over two-and-a-half years with work resulting in two journal publications, three conference publications, and a patent. Some of his work was featured in general audience literature such as *Business Week*, *Discover Magazine*, and others. He still pursues this research in his spare time as a hobby. He also was a member of the University of Michigan Synthetic Biology Team and presented work from a project of his design at the 2008 Internationally Genetically Engineered Machine Competition at MIT (iGEM).

In June of 2008, Mr. Steinmeyer joined the research group of Associate Professor Mehmet Fatih Yanik which applies state of the art technology problems to fundamental problems in biology and neuroscience. Since late 2008, he has been pursuing work, some of which is presented in this paper, focusing on a means to rapidly transfect multiple labeling agents into organotypic brain slices. He is currently supported by the National Defense Science and Engineering Graduate Fellowship (NDSEG) and is also a recipient of the National Science Foundation Graduate Research Fellowship Program (NSFGRF).

APPENDIX A. SOLUTIONS AND MEDIA:

Slicing Media and Bath Solution:

25 mM HEPES dissolved in EBSS

Culture Media[12] *(for ~100 mL):*

50 mL MEM with Glutamax-1
18 mL EBSS
25 mL Horse Serum
36 mM D-Glucose
Streptomycin/Penicillin 0.08 mM
60 µL Nystatin

Ringer Solution[14]*:*

135 mM NaCl
5.4 mM KCl
1 mM $MgCl_2$
1.8 mM $CaCl_2$
5 mM HEPES

Plasmids were stored at 4°C in DI water until use at which point they were buffered to approximately pH = 7.4.

APPENDIX B. PHOTOGRAPH OF AUTOMATED SINGLE-CELL ELECTROPORATION SYSTEM

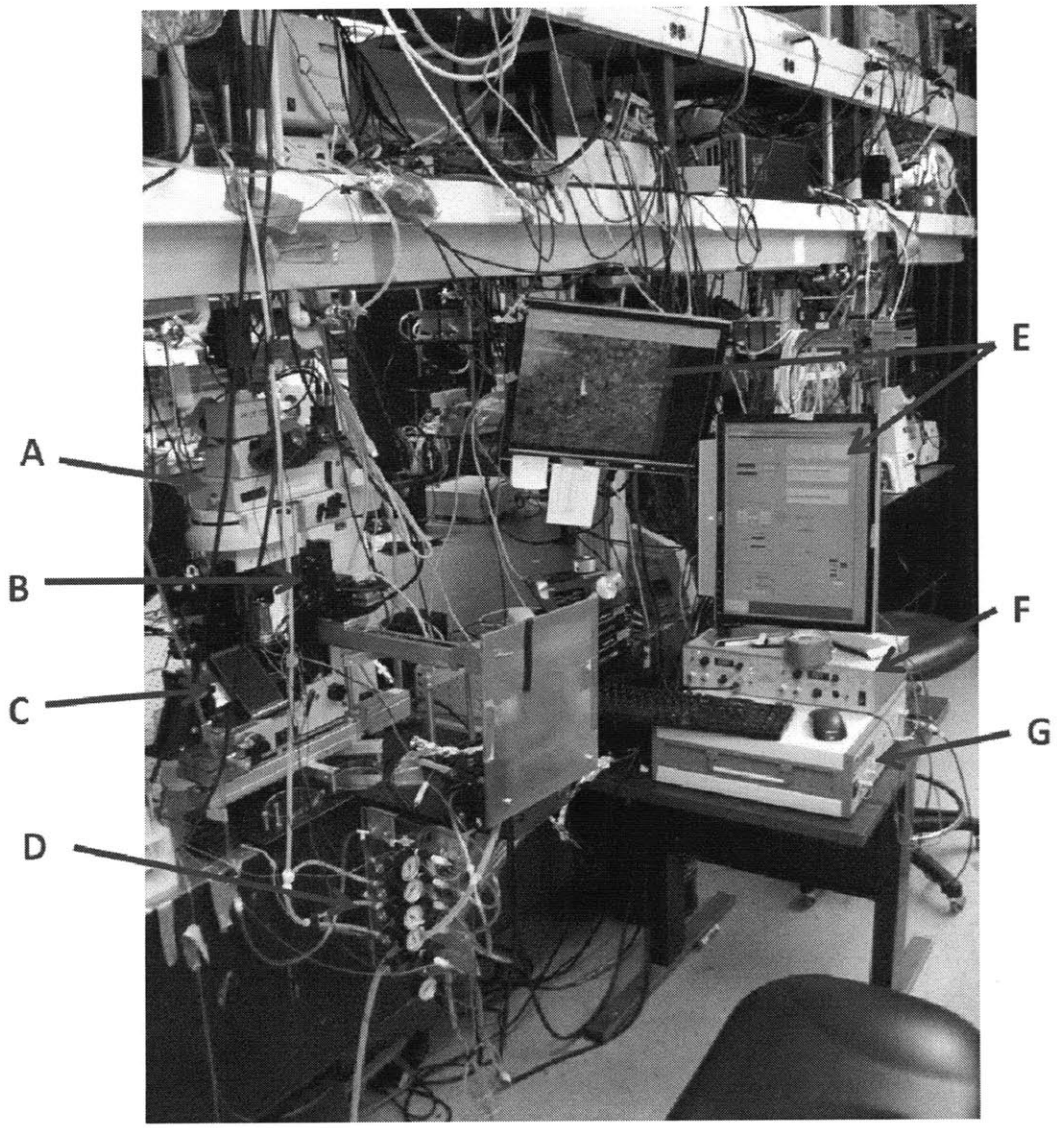

Figure AB1. The FN-1 microscope (**A**), the micromanipulator controlling the micropipette (**B**), the well-plate containing samples (**C**), the pressure/vacuum control and regulation (**D**), Computer monitors depicting the software running with micropipette inserted into brain tissue (**E**), the temperature controller (**F**), and the high-voltage amplifier (**G**).

APPENDIX C. NOTES ON SOFTWARE DEVELOPED

During the course of the system development, it was discovered that Sutter Instruments does not provide MATLAB-compatible interface files for USB usage of its MPC-200 or SmartShutter™ line of equipment. Chris Rohde previously developed control code for the SmartShutter™ line, and I developed a library of MATLAB commands for the Sutter MPC-200 and MP 285 micromanipulator

For the long-travel stages built by IAI, I wrote a library of commands that be easily called from MATLAB, as well using serial port commands.

In the interests of the greater scientific community, both of these command libraries are available to any interested parties and can be obtained by contacting the author at jodalyst@mit.edu

REFERENCES

1. Pfrieger, F.W. Role of glia in synapse development. *Current Opinion in Neurobiology* **12**, 486-490 (2002).
2. Barres, B.A. The Mystery and Magic of Glia: A Perspective on Their Roles in Health and Disease. *Neuron* **60**, 430-440 (2008).
3. Duff, K., Noble, W., Gaynor, K. & Matsuoka, Y. Organotypic Slice Cultures from Transgenic Mice as Disease Model Systems. *Journal of Molecular Neuroscience* **19**, 317-320 (2002).
4. Prieto, P., *et al.* The Assessment of Repeated Dose Toxicity *In Vitro:* A Proposed Approach. *ATLA* **34**, 315-341 (2006).
5. Vogel, A., Noack, J., Huttman, G. & Paltauf, G. Mechanisms of femtosecond laser nanosurgery of cells and tissues. *Applied Physics B-Lasers and Optics* **81**, 1015-1047 (2005).
6. Gogolla, N., Galimberti, I., DePaola, V. & Caroni, P. Long-term live imaging of neuronal circuits in organotypic hippocampal slice cultures. *Nature Protocols* **1**, 1223-1226 (2006).
7. Walsh, K., Megyeshi, J. & Hammond, R. Human central nervous system tissue culture: a historical review and examination of recent advances. *Neurobiology of Disesase* **18**, 2-18 (2005).
8. Gahwiler, B.H. Organotypic monolayer cultures of nervous tissue. *Journal of Neuroscience Methods* **4**, 329-342 (1981).
9. Gahwiler, B.H. Organotypic cultures of neural tissue. *Trends in Neurosciences* **11**, 484-489 (1988).
10. Stoppini, L., Buchs, P.-A. & Muller, D. A simple method for organotypic cultures of nervous tissue. *Journal of Neuroscience Methods* **37**, 173-182 (1991).
11. Gogolla, N., Galimberti, I., DePaola, V. & Caroni, P. Preparation of organotypic hippocampal slice cultures for long-term imaging. *Nature Protocols* **1**, 1165-1171 (2006).
12. De Simoni, A. & Yu, L.M. Preparation of organotypic hippocampal slice cultures: interface method. *Nature Protocols* **1**, 1439-1445 (2006).
13. De Simoni, A., Griesinger, C.B. & Edwards, F.A. Development of rat CA1 neurones in acute versus organotypic slices: role of experience in synaptic morphology and activity. *Journal of Physiology* **550**, 135-147 (2003).
14. Rathenberg, J., Nevian, T. & Witzemann, V. High-efficiency transfection of individual neurons using modified electrophysiology techniques. *Journal of Neuroscience Methods* **126**, 91-98 (2003).
15. Wang, W., Qu, Q., Smith, F.I. & Kilpatrick, D.L. Self-inactivating lentiviruses: Versatile vectors for quantitative transduction of cerebellar granule neurons and their progenitors. *JOurnal of Neuroscience Methods* **149**, 144-153 (2005).
16. Song, C.K., Enquist, L.W. & Bartness, T.J. New developments in tracing neural circuits with herpesviruses. *Virus Res.* **111**, 235-249 (2005).
17. Teschemacher, A.G., *et al.* Targeting specific neuronal populations using adeno- and lentiviral vectors: applications for imaging studies of cell function. *Experimental Physiology* **90**, 61-69 (2004).
18. Kasri, N.N., Govek, E.-E. & Aelst, L.V. Chapter Nineteen: Characterization of Oligophrenin-1, a RhoGAP Lost in Patients Affected with Mental Retardation: Lentiviral Injection in Organotypic Brain Slice Cultures. *Methods in Enzymology* **439**, 255-266 (2008).
19. Zhang, Y. & Yu, L.-C. Single-cell microinjection technology in cell biology. *BioEssays* **30**, 606-610 (2008).
20. Komarova, Y., Peloquin, J. & Borisy, G. Preparation and Loading of Protein Samples for Microinjection. *Cold Spring Harbor Protocols* (2007).
21. Schneckenburger, H., Hendinger, A., Sailer, R., Strauss, W.S.L. & Schmitt, M. Laser-assisted optoporation of single cells. *Journal of Biomedical Optics* **7** (2002).
22. Nugent, E.M. Optoporation: Laser-Assisted Permeation of Vertebrate Cell Membranes. in *Physics* (The College of William and Mary, Williamsburg, VA, 2006).
23. Chen, C., Smye, S.W., Robinson, M.P. & Evans, J.A. Membrane electroporation theories: a review. *Medical and Biological Engineering and Computing* **44**, 5-14 (2006).

24. Olofsson, J., *et al.* Single-cell electroporation. *Current Opinion in Biotechnology* **14**, 29-34 (2003).
25. Saito, T. & Nakatsuji, N. Efficient Gene Transfer into the Embryonic Mouse Brain Using *in Vivo* Electroporation. *Developmental Biology* **240**, 237-246 (2001).
26. Ionescu-Zanetti, C., Blatz, A. & Khine, M. Electrophoresis-assistend single-cell electroporation for efficient intracellular delivery. *Biomedical Microdevices* **10**, 113-116 (2008).
27. Khine, M., Lau, A., Ionescu-Zanetti, C., Seo, J. & Lee, L.P. A single cell electroporation chip. *Lab on a Chip* **5**, 38-43 (2004).
28. Mudgett, J.S. & Livelli, T.J. Electroporation of Embryonic Stem Cells for Generating Transgenic Mice and Studying In Vitro Differntiation. in *Animal Cell Electroporation and Electrofusion Protocols* 167-184 (Springer, 1995).
29. Doh, S.T., *et al.* Analysis of retinal cell development in chick embryo by immunohistochemistry and *in ovo* electroporation techniques. *BMC Developmental Biology* **10** (2010).
30. Uesaka, N., Hayano, Y., Yamada, A. & Yamamoto, N. Single Cell Electroporation Method for Mammalisan CNS Neurons in Organotypic Slice Cultures. in *Electroporation and Sonoporation in Developmental Biology* 169-177 (Springe Japan, 2009).
31. Lundqvist, J.A., *et al.* Altering the biochemical state of individual cultured cells and organelles with ultramicroelectrodes. *Proceedings of the National Academy of the Sciences USA* **95**, 10356-10360 (1998).
32. Ryttsén, F., *et al.* Characterization of Single-Cell Electroporation by Using Patch-Clamp and Fluorescence Microscopy. *Biophysical Journal* **79**, 1993-2001 (2000).
33. Nolkrantz, K., *et al.* Electroporation of Single Cells and Tissues with an Electrolyte-filled Capillary. *Analytical Chemistry* **73**, 4469-4477 (2001).
34. Haas, K., Sin, W.-C., Javaherian, A., Li, Z. & Cline, H.T. Single-Cell Electroporation for Gene Transfer in Vivo. *Neuron* **29**, 583-591 (2001).
35. Bae, C. & Butler, P.J. Automated single-cell electroporation. *BioTechniques* **41**, 399-402 (2006).
36. Kitamura, K., Judkewitz, B., Kano, M., Denk, W. & Häusser, M. Targeted patch-clamp recordings and single-cell electroporation of unlabeled neurons *in vivo*. *Nature Methods* **5**, 61-67 (2008).
37. Judkewitz, B., Rizzi, M., Kitamura, K. & Häusser, M. Targeted single-cell electroporation of mammalian neurons *in vivo*. *Nature Protocols* **4**, 862-869 (2009).
38. Lovell, P., Jezzini, S.H. & Moroz, L.L. Electroporation of neurons and growth cones in *Aplysia californica*. *Journal of Neuroscience Methods* **151**, 114-120 (2006).
39. Bestman, J.E., Ewald, R.C., Chiu, S.-L. & Cline, H.T. *In vivo* single-cell electroporation for transfer of DNA and macromolecules. *Nature Protocols* **1**, 1267-1272 (2006).
40. Tanaka, M., Yanagawa, Y. & Hirashima, N. Transfer of small interfering RNA by single-cell electroporation in cerebellar cell cultures. *Journal of Neuroscience Methods* **178**, 80-86 (2009).
41. Blomberg, P., Eskandarpour, M., Xia, S., Sylven, C. & Islam, K.B. Electroporation in combination with a plasmid vector containing SV40 enhancer elements results in increased and persistent gene expression in mouse muscle. *Biochemical and Biophysical Research Communications* **298**, 505-510 (2002).
42. Gehl, J. Electroporation: theory and methods, perspectives for drug delivery, gene therapy and research. *Acta Physiology Scandanavia* **177**, 437-447 (2003).
43. Zudans, I., Agarwal, A., Orwar, O. & Weber, S.G. Numerical Calculations of Single-Cell Electroporation with an Electrolyte-Filled Capillary. *Biophysical Journal* **92**, 3696-3705 (2007).
44. Wang, M., Orwar, O. & Weber, S.G. Single-Cell Transfection by Electroporation Using an Electrolyte/Plasmid-Filled Capillary. *Analytical Chemistry* **81**, 4060-4067 (2009).
45. Rols, M.P. & Teissie, J. Electropermeabilization of Mammalian Cells to Macromolecules: Control by Pulse Duration. *Biophysical Journal* **75**, 1415-1423 (1998).
46. Steinmeyer, J.D., *et al.* Construction of a femtosecond laser microsurgery system. *Nature Protocols* **5**, 395-407 (2010).

47. Brown, K.T. & Flaming, D.G. *Advanced Micropipette Techniques for Cell Physiology* (Wiley-Interscience, Chichester, 1986).
48. Schellman, J.A. Electrical Double Layer, Zeta Potential, and Electrophoretic Charge of Double-Stranded DNA. *Biopolymers* **16**, 1415-1434 (1977).
49. Gu, Y. & Li, D. The Zeta-Potential of Glass Surface in Contact with Aqueous Solutions. *Journal of Colloid and Interface Science* **226**, 328-339 (2000).
50. Sze, A., Erickson, D., Ren, L. & Li, D. Zeta-Potential measurement using the Smoluchoswki equation and the slope of the current-time relationship in electroosmotic flow. *Journal of Colloid and Interface Science* **261**, 402-410 (2003).
51. Evenhuis, C.J., Guijt, R.M., Macka, M., Marriott, P.J. & Haddad, P.R. Variation of zeta-potential with temperature in fused-silica capillaries used for capillary electrophoresis. *Electrophoresis* **27**, 672-676 (2006).
52. Weinberger, R. *Practical Capillary Electrophoresis* (Academic Press, Inc., San Diego, CA, 2000).
53. Righetti, P.G. *Capillary Electrophoresis in Analytical Biotechnology* (CRC Press, New York, 1996).
54. Jandik, P. & Bonn, G. *Capillary Electrophoresis of Small Molecules and Ions* (VCH Publishers, Inc., New York, 1993).
55. Grossman, P.D. & Colburn, J.C. *Capillary Electrophoresis: Theory & Practice* (Academic Press, Inc., San Diego, CA, 1992).
56. Nitsche, J.M., Chang, H.-C., Weber, P.A. & Nicholson, B.J. A Transient Diffusion Model Yields Unitary Gap Junctional Permeabilities from Images of Cell-to-Cell Fluorescent Dye Transfer Between Xenopus Oocytes. *Biophysical Journal* **86**, 2058-2077 (2004).
57. Prazeres, D.M.F. Prediction of Diffusion Coefficients of Plasmids. *Biotechnology and Bioengineering* **99**, 1040-1044 (2007).
58. Carmejane, O., Schwinefus, J.J., Wang, S.-C. & Morris, M.D. Electrophoretic separation of linear and supercoiled DNA in uncoated capilaries. *Journal of Chromatography A* **849**, 267-276 (1999).
59. Boudes, M., Pieraut, S., Valmier, J., Carroll, P. & Scamps, F. Single-cell electroporation of adult sensorty neurons for gene screening with RNA interference mechanism. *Journal of Neuroscience Methods* **170**, 204-211 (2008).
60. Uesaka, N., Nishiwaki, M. & Yamamoto, N. Single cell electroporation method for axon tracing in cultured slices. *Development, Growth, and Differentiation* **50**, 475-477 (2008).
61. Lyman, W., *et al.* HIV-1 infection of human fetal central nervous system organotypic cultures. in *International Conference on AIDS* (1989).
62. Lyman, W.D., *et al.* Human fetal central nervous system organotypic cultures. *Brain Research, Developmental Brain Research* **60**, 155-160 (1991).
63. Bauer, M., *et al.* Liposome-mediated gene transfer to fetal human ventral mesencephalic explant cultures. *Neuroscience Letters* **308**, 169-172 (2001).
64. Letinic, K., Zoncu, R. & Rakic, P. Origin of GABAergic neurons in the human neocortex. *Nature* **417**, 645-649 (2002).
65. Verwer, R.W., Dubelaar, E.J., Hermens, W.T. & Swaab, D.F. Tissue culture from adult human postmortem subcortical brain areas. *Journal of Cell and Molecular Medicine* **6**, 429-432 (2002).
66. Verwer, R.W., *et al.* Post-mortem brain tissue cultures from elderly control subjects and patients with a neurodegenerative disease. *Experimental Gerontology* **38**, 167-172 (2003).
67. Vostrikov, V.M., *et al.* Organotypic Cultures of Free-Floating Slices of Human Embryo Medulla Oblongata. *Neuroscience and Behavioral Physiology* **35**, 9-15 (2005).

This research was supported by grants from the National Institutes of Health and by the MIT Department of Electrical Engineering and Computer Science. Joseph Steinmeyer was supported by the National Defense Science and Engineering Graduate Fellowship funded by the Department of Defense and administered by the American Society for Engineering Education, as well as the National Science Foundation Graduate Research Fellowship.